University of Alberta

Factors influencing glucose homeostasis in a rat model with mutated ATP synthase.

by

Anne Catherine Harasym

A thesis submitted to the Faculty of Graduate Studies and Research
in partial fulfillment of the requirements for the degree of

Master of Science
in
Nutrition & Metabolism

Department of Agricultural, Food & Nutritional Sciences

Spring 2012
Edmonton, Alberta

Abstract

This study examined glucose homeostasis mechanisms involved in the BHE/cdb rat model of mitochondrial diabetes with a mutated F_o subunit of ATP synthase. Twenty-one-week old male BHE/cdb rats exhibited enhanced glucose tolerance despite impaired insulin secretion. Whole body *in vivo* characterization showed that BHE/cdb rats had enhanced insulin sensitivity compared to controls, along with moderately increased ($p<0.01$) respiratory exchange ratios, oxygen consumption, carbon dioxide production and heat production, despite similar relative body composition, physical activity, food and water consumption. *In vitro* markers of insulin-dependent and insulin-independent signaling pathways were similar in BHE/cdb rats and controls. Phosphoenolpyruvate carboxykinase expression in liver ($p<0.05$), liver glycogen storage ($p<0.05$), and epitrochlearis muscle glycogen ($p<0.01$) were increased in BHE/cdb rats. Additionally, *in vivo* pyruvate-stimulated gluconeogenesis was attenuated in BHE/cdb rats ($p<0.01$). Results indicate that increased glucose oxidation, increased thermogenesis, and reduced hepatic glucose output mediate glucose tolerance in the BHE/cdb model.

Acknowledgements

The completion of this thesis would not be a reality without the contributions from many different people. First off, I would like to thank my supervisor Dr. Cathy Chan. Her understanding, encouragement and positive feedback in the face of multiple mistakes, delays and unexpected problems throughout my two years at the University of Alberta has been invaluable. Also, thanks to my co-supervisor Dr. David Wright, for helping start my degree off on the right foot. Starting from the email I sent when applying to graduate school to showing me the ropes in the lab, he too has been nothing but encouraging and enthusiastic, despite moving across the country. This process has been much smoother than I had anticipated with their help and dedication. I would also like to thank my committee member, Dr. Chris Cheeseman, for taking the time to help me out with some of his excellent research experience, as well as Dr. Rene Jacobs, for his contributions regarding pyruvate tolerance testing and lipid extractions.

All of the members of the Chan lab, especially Dr. Zahra Fatehi-Hassanabad, Zohre Hashemi, Nicole Coursen, Lisa Kocizky, Homun Yee, Kevin Whitlock & Ghada Asaad; their help with my experiments, feedback on posters and presentations, as well as some excellent pot-luck food has been very much appreciated. In addition, thanks to all of the former members of the U of A Wright lab: Dr. Bruce Frier, Deon Williams, Mélanie Légaré, and Caroline Wan, for teaching me everything I needed to know about western blotting.

I would like to acknowledge the financial support of NSERC and the Alberta Diabetes Institute for personal funding, as well as NSERC for project funding.

Last, but certainly not least, I would like to express gratitude to my friends and family who put up with me while I was “thesising”, thanks.

Table of Contents

List of Tables

List of Figures

List of Abbreviations

ACC	acetyl CoA carboxylase
AIF	apoptosis inducing factor
Akt	protein kinase B (PKB)
AMPK	5' adenosine monophosphate-activated protein kinase
ANOVA	analysis of variance
ADP	adenosine diphosphate
AMP	adenosine monophosphate
AS160	Akt substrate of 160 kDa
ATP	adenosine triphosphate
AUC	area under the curve
BCA	bicinchoninic acid (assay)
BHE	BHE/cdb, Bureau of Home Economics
BSA	bovine serum albumin
CaMKK	calmodulin-dependent protein kinase kinase
CDA	Canadian Diabetes Association
CLAMS	comprehensive lab animal monitoring system
CO_2	carbon dioxide
CV	calorific value
dH_2O	distilled water
DNA	deoxyribonucleic acid
DTT	dithiothreitol
ELISA	enzyme-linked immunosorbent assay
EtBr	ethidium bromide
F_1F_oATPase	ATP synthase, consisting of F_1 and F_o subunits
FoxO1	forkhead box protein O1

G6P	glucose -6- phosphatase
GAPDH	glyceraldehyde-3-phosphate dehydrogenase
GC	gas-liquid chromatography
GLUT4	glucose transporter 4
GSK3	glycogen synthase kinase -3
HFD	high fat diet
HRP	horseradish peroxidase
ip.	intraperitoneal
ipGTT	intraperitoneal glucose tolerance test
IR	insulin receptor
IRS	insulin receptor substrate
ITT	insulin tolerance test
kDa	kilodalton
Leu	leucine, amino acid residue
LKB1	liver kinase B1
MAPK	Ras-mitogen-activated protein kinase
Mef2	myocyte enhancer factor 2
MIDD	maternally inherited diabetes and deafness syndrome
MnSOD	manganese superoxide dismutase
MRI	magnetic resonance imaging
mtDNA	mitochondrial deoxyribonucleic acid
N_2	nitrogen
NIH	National Institutes of Health
O_2	oxygen
PDH	pyruvate dehydrogenase
PDK1	3-phosphoinosite-dependent protein kinase 1

PEPCK	phosphoenolpyruvate carboxykinase
PGC-1α	peroxisome proliferative activated receptor-γ co-activator 1
PI3K	phosphatidylinositol 3-kinase
PIP_3	phosphatidylinositol-3,4,5-triphosphate
PKB	protein kinase B (Akt)
PTT	pyruvate tolerance test
RER	respiratory exchange ratio (also known as RQ)
ROS	reactive oxygen species
RQ	respiratory quotient (also known as RER)
SD	Sprague Dawley
SDS-PAGE	sodium dodecyl sulfate polyacrylamide gel electrophoresis
SE	standard error
Ser	serine, amino acid residue
T1D	type 1 diabetes mellitus
T2D	type 2 diabetes mellitus
TBST	tris-buffered saline with 0.1% Tween 20
Tfam	mitochondrial transcription factor A
Thr	threonine, amino acid residue
TORC2	transcriptional regulator transducer of regulated cAMP-response element binding protein activity 2 – also known as CRTC2 – CREB regulated transcription co activator 2
tRNA	transfer ribonucleic acid
UCP3	uncoupling protein 3
VCO_2	volume of carbon dioxide produced
VO_2	volume of oxygen consumed
w/v	weight per unit volume
w/w	weight per unit weight

1.0 Literature Review

1.1 Introduction to Diabetes Mellitus

Diabetes mellitus, a metabolic disorder characterized by hyperglycemia due to the body's inability to properly produce or use insulin, is one of the world's most common chronic diseases (Canadian Diabetes Association [CDA], 2008). Long-term health complications, including damage to the cardiovascular system, eyes, kidneys, and nerves, which occur as a result of diabetes mellitus induced hyperglycemia present a significant impact on global population health. The estimated global prevalence of diabetes is 8.3 %, affecting 366 million people in 2011. Meanwhile, in Canada, diabetes prevalence in 2011 is estimated to be 10.8%, with an estimated 2.7 million adults living with diabetes (Whiting *et al.*, 2011).

Diabetes is classified into two main forms, type 1 diabetes (T1D) and type 2 diabetes (T2D). In T1D, the body can no longer produce insulin primarily due to autoimmune destruction of pancreatic β-cell destruction. In T2D, hyperglycemia occurs as a result of a combination of either impaired insulin production or secretion and the inability of the body's tissues to respond to insulin (CDA, 2008). A wide range of genetic, developmental, lifestyle and environmental factors can contribute to the development of T2D. In general, the genetic component of common T2D is polygenic, or can be attributed to multiple genetic mutations in a given individual. However, a small subset of T2D, accounting for no more than an estimated 2%-5% of T2D cases, are considered to be monogenic and occur as a result of a single genetic mutation (Doria *et al.,* 2008). Mitochondrial diabetes is a monogenic form of diabetes in humans that can arise from a single mutation in

either the mitochondrial DNA (mtDNA) or nuclear DNA that affects β-cell mitochondrial function (Schiff *et al.,* 2009).

1.2 Metabolic Regulation and Glucose Homeostasis

The proper regulation of metabolic processes in the body results in homeostasis. Homeostasis is the maintenance of the balance or stability of physiology within the body to ensure optimum function. Changes in homeostasis due to irregular or aberrant metabolism often result in disease, such as is seen in the changes in glucose homeostasis that is characteristic of diabetes mellitus. Therefore, the role of energy homeostasis with respect to glucose and its regulators is important in understanding specific components of the diabetic disease process.

The control of plasma glucose levels is a complex process that balances whole body glucose production and glucose utilization through multiple tissues, hormones, and counter-regulatory feedback loops in fed and fasted states. In general, following ingestion of a meal, plasma glucose rises. Upon detection of elevated plasma glucose, pancreatic β-cells are stimulated to synthesize and secrete insulin. Insulin synthesis and secretion from the β-cell are regulated by the presence of adenosine triphosphate (ATP)(Matchinsky, 1996). While insulin has a wide range of effects on the body, its main action is to promote the uptake of glucose from the blood into skeletal muscle and adipose tissue and suppress hepatic glucose output (Schiff *et al.,* 2009). Hepatic glucose regulation by insulin includes the inhibition of glycolysis, the promotion of glycogen synthesis and storage, as well as the inhibition of gluconeogenesis (Cherrington, 1999; Roden *et al.,* 2001). Conversely, upon detection of hypoglycemia, a counter-regulatory response is generated to

promote an increase in blood glucose levels. For example, in an acute hypoglycemic state, glucagon is secreted from the α-cells of the pancreas and is responsible for stimulating gluconeogenesis and glycogenolysis in the liver, which then releases glucose into the blood to be used by other tissues (Cherrington, 1999). Homeostasis of blood glucose ensures that cells have access to an adequate energy source to produce ATP to maintain normal functions.

The use and synthesis of the high-energy compound ATP is central in the normal control of metabolism. ATP can be produced via direct substrate phosphorylation of adenosine diphosphate (ADP), such as occurs in glycolysis. However, most ATP is produced in the mitochondria via oxidative phosphorylation (Berdanier, 2001). Oxidative phosphorylation is the process which captures energy generated from breakdown of pyruvate in the citric acid cycle and the subsequent reduction reactions in the mitochondrial respiratory chain to synthesize ATP. ATP synthase is the final protein complex which couples the movement of protons from the inter-membrane space across the inner mitochondrial membrane into the mitochondrial matrix to catalyze the synthesis of ATP from inorganic phosphate and ADP (Berdanier, 2001). ATP can be used in a wide variety of energy-requiring processes within the cell, making it evident that the proper functioning of mitochondria is important in whole-body homeostasis.

1.3 Mitochondrial Diabetes in Humans

The transcription of proteins involved in mitochondrial oxidative phosphorylation is controlled by genes present in both nuclear DNA and mitochondrial DNA. Genes present in mtDNA encode for 13 polypeptides which are subunits of proteins

involved in oxidative phosphorylation, 22 transfer RNAs (tRNA), as well as two ribosomal RNAs (Park & Larsson, 2011). In humans, mitochondrial diabetes was first identified by its maternal mode of inheritance associated with a point mutation in mtDNA and described as a subtype of T2D called maternally inherited diabetes and deafness syndrome (MIDD)(van den Ouweland *et al.,* 1992; Maassen & Kadowaki, 1996). Maternal inheritance patterns are seen with mtDNA mutations because paternal mitochondria are not retained in a fertilized oocyte (Maassen, 2002).

The phenotype of maternally inherited mitochondrial diseases such as MIDD is very heterogeneous. There are multiple copies of mtDNA per cell, as there are many mitochondria within each individual cell and multiple copies of mtDNA within each mitochondrion (Wallace, 1999). Mitochondrial DNA is highly susceptible to mutation and the mtDNA mutations within a cell may not occur in all copies of mtDNA, resulting in mtDNA heteroplasmy. The majority of pathogenic mtDNA mutations appear to account for only a small fraction of the total mtDNA, rather than being homoplasmic in nature (Wallace, 1999). This phenomenon can be attributed to the fact that a mutation which does not impact mitochondrial function can survive multiple cell divisions and eventually become the only mutation present, whereas a pathogenic mutation would not survive as many cell divisions and are therefore usually present in higher number in cells which do not undergo rapid cellular division, such as skeletal muscle (Maassen, 2002). Traditionally, tissue with high heteroplasmy of pathogenic mtDNA mutations, such as muscle, also have a high energy demand, thus resulting in sensitivity to the

availability of ATP, the end product of mitochondrial oxidative phosphorylation (Maassen, 2005).

MIDD has been associated with the biochemical consequences due to the 3243A<G mutation in the mtDNA gene encoding for mitochondrial transfer ribonucleic acid (tRNA)(*Leu*, UUR), which has been shown to account for a 70% reduction in oxygen consumption in mitochondria in patients with a high number of the A3243G mutations present (van den Ouweland *et al.*, 1992; Maassen, 2002). This mutation impairs encoding of proteins from mtDNA, resulting in impaired production of ATP from oxidative phosphorylation (Maassen, 2002). Other point mtDNA mutations have been identified and associated with increased risk of diabetes. However, these mutations occur at a much lower frequency than the A3243G mutation (Maassen *et al.,* 2005). It was initially hypothesized that diabetes in this population was mainly related to peripheral insulin resistance; however, it has since been shown that most carriers of the A3243G mutation do not exhibit peripheral insulin resistance, despite evidence of impaired mitochondrial oxidative phosphorylation after exercise in A3243G mutation carriers (Maassen *et al.,* 2004; van Elderen *et al.,* 2009). Aging, combined with a decrease in glucose-induced insulin secretion by the pancreatic β-cell, has been indicated as the main link between the A3243G mutation and diabetes in human mitochondrial diabetes (Maassen *et al.,* 2005). Upon aging, most A3243G mutation carriers will show an accelerated decline in insulin secretion, especially when associated with other lifestyle risk factors, such as obesity, and by age 70 approximately 85% of carriers will develop diabetes (Brandle, *et al.,* 2001; Maassen, *et al.,* 2005). While the development of diabetes in the A3243G mutation carrying population can be

attributed to a combination of many different factors, such as the excess production of reactive oxidative species and lipid-induced toxicity in the β-cell, the exact mechanisms by which the A3243G mutation inhibits β-cell glucose sensing, insulin production or insulin secretion remains inconclusive (Maassen *et al.,* 2004).

1.4 Models of Mitochondrial Diabetes

Animal models and cell culture experiments have been identified and developed to help further understand the interaction between mitochondrial defects and the development of diabetes. Manipulation of nuclear DNA in animal models is relatively easy, such as by using recombination with specifically generated DNA sequences and breeding to produce gene knockouts or silencing using short interfering RNA to produce gene knockdowns. However, direct manipulations of mtDNA are not feasible in animal models, making it difficult to study specific mtDNA mutations in humans (de Andrade *et al.,* 2006). Therefore, a number of models were developed to look at mtDNA depletion and its effect on β-cell function and the development of diabetes. Kennedy *et al.* (1998) used ethidium bromide (EtBr) to deplete mtDNA in the INS-1 cell line and evaluated the effect of loss of mtDNA on insulin secretion and cell function. Upon treatment with EtBr, the ability of the differentiated β-cells to produce ATP upon glucose stimulation was abolished due to defects in mitochondrial function, but had no effect on insulin exocytosis from the cell when stimulated independent of nutrient secretagogues. This work shows that the presence of mtDNA is essential for glucose-stimulated insulin secretion.

Other cell culture experiments looking specifically at cell lines generated from human patients with the A2343G mutation were conducted by de Andrade and colleagues (2006). A human osteocarcoma cell line was used to introduce mitochondria derived from human A3243G mutation carriers and wild type controls to create cybrid cell cultures. The cybrids containing the A3243G mutation demonstrated decreased ATP generation, decreased glucose oxidation as well as increased levels of reactive oxygen species, demonstrating impairments in metabolic pathways crucial to the maintenance of normal blood glucose.

A mouse model of mitochondrial diabetes was generated through the pancreatic β-cell specific knockout of the nuclear gene encoding for mitochondrial transcription factor A (Tfam) (Silva *et al.,* 2000). Tfam is a transcriptional activator that is essential for the maintenance and expression of mtDNA, and therefore the mutant strain developed diabetes a young age. The diabetic state in the Tfam deficient mice was accompanied by deficient oxidative phosphorylation as well as impaired glucose-stimulated insulin secretion. Interestingly however, when subjected to insulin tolerance tests, these mice showed enhanced insulin sensitivity with age, indicating that peripheral tissues may have undergone compensatory adaptation in response to impaired β-cell function (Silva *et al.,* 2000). This work furthered evidence of the importance of the proper functioning of the respiratory chain in insulin secretion and maintenance of normal blood glucose.

An animal model that has been identified to have a milder form of mitochondrial diabetes that may more closely resemble the progression of mitochondrial diabetes in the human population is the BHE/cdb rat (Berdanier, 2007). The

BHE/cdb strain has been used to evaluate the impact of diet on the progression of diabetes in a progressive non-obese model in numerous studies by Berdanier and colleagues (Berdanier, 2007; Berdanier *et al.,* 1992; Everts & Berdanier, 2002). The BHE/cdb rat was bred specifically to develop impaired glucose tolerance at midlife originating from a mixed-background colony. Selective breeding pressure was placed on the maternally inherited traits of rats with fatty liver and impaired glucose tolerance in order to generate a substrain that developed abnormal glucose tolerance by approximately 300 days of age (Berdanier, 2007). The impaired glucose tolerance is a characteristic of the progression of T2D in which the pancreas is unable to secrete sufficient insulin in response to an oral dose of glucose to remove glucose from the blood into peripheral tissues. In addition to abnormal glucose tolerance, these rats displayed other metabolic abnormalities including decreased efficiency of ATP synthesis (Berdanier & Thomson, 1986). The BHE/cdb β-cells from isolated pancreatic islets were subsequently shown to have reduced glucose-stimulated insulin secretion with aging, which was associated with decreased ATP levels (Liang *et al.,* 1994; Matchinsky, 1996). However, it was seen in these studies that the defect in these β-cells was not related to decreased glucose uptake or glucokinase activity, indicating that the primary defect in this strain was not in β-cell glucose transport (Liang *et al.,* 1994).

Point mutations in the mitochondrial gene that encodes ATP synthase (F_1F_oATPase) in the BHE/cdb rat were identified in the ATPase gene 6 for the expression of subunit *a* of the F_o portion of F_1F_oATPase (Mathews *et al.,* 1995). The mutation at bp8204 causes a codon change from directing the addition of an aspartic acid residue to directing an asparagine residue in the membrane-spanning

F_o portion of ATP synthase, which mediates proton flow (Berdanier, 2007). A change in the polarity of this channel could reduce the efficiency of energy capture from proton movement and thus impede ADP phosphorylation to ATP by the F_1 portion of ATP synthase (Mathews *et al.,* 1995; Berdanier, 2001). Additionally, a second substitution at bp8289 translates at a hinge-like structure of the F_oATPase section. This substitution affects the flexibility of the molecule in the membrane, which has been hypothesized to be the site at which changes in membrane fluidity, caused by changes in dietary fat intake, could influence ATP synthesis (Mathews *et al.,* 1995; Berdanier, 2007). Further genetic analysis was conducted to confirm the association between the mitochondrial defect and impaired glucose tolerance. Interestingly, in all tissues tested the BHE/cdb rats showed mtDNA homeoplasmy for the F_oATPase subunit *a* mutations, unlike most mutations associated with mitochondrial diabetes seen in humans (Mathews *et al.,* 1999; Wallace, 1999). The maternally inherited mutations were confirmed to associate with age-related impaired glucose tolerance (Mathews *et al.,* 1999).

The mtDNA mutations causing proton leak and reduced efficiency of ATP synthesis in the BHE/cdb rat can be considered analogous to two mutations identified in humans, either a T8993G or a T8993C mutation in the ATPase 6 gene (Berdanier 2007; Vazquez-Memije *et al.,* 1998). Each causes a change in polarity of the F_o portion of ATP synthase resulting in impaired ATP synthesis. In humans with the T8993G mutation, which impedes ATP synthesis to a greater extent than the T8993C mutations, the arginine is substituted for leucine, while, as previously mentioned, in the BHE/cdb rats asparagine is substituted for aspartic acid. Therefore, the BHE/cdb rat is an interesting model in which to relate changes in

ATP availability to the metabolic parameters associated with diabetes, but further characterization of the influence of ATP in peripheral glucose metabolism in this model is required.

1.5 Molecular Mechanisms in Insulin Signaling

As discussed previously, insulin is the primary hormone regulating blood glucose levels through stimulation of glucose influx into muscle and adipocytes and the inhibition of liver glucose output (White & Kahn, 1994). Insulin action throughout the body is highly regulated on a molecular level by complex and inter-related cell signaling cascades. When insulin is secreted from the pancreas into the blood stream the hormone does not enter cells, but acts on receptor molecules on the surface of cellular membranes to effect action within a cell (Avurch, 1998). Intracellular signaling cascades can be regulated though changes in the phosphorylation state of effector proteins, which result in either activation or inhibition of a substrate protein. Simplistically speaking, in the presence of insulin, the membrane-spanning tyrosine insulin receptor (IR) proteins on the surface of cell membranes phoshporylate insulin receptor substrate proteins (IRS proteins) within the cell. Phosphorylated IRS proteins then activate two main signaling pathways: the metabolic regulatory phosphatidylinositol 3-kinase (PI3K)-Akt/protein kinase B (PKB) pathway and the Ras-mitogen-activated protein kinase (MAPK) pathway, which is involved in the regulation of gene expression, cell growth and differentiation (Taniguchi *et al.,* 2006). The focus of this thesis project relates more closely to the downstream effects of the PI3K-Akt/PKB, so it will be reviewed in more detail than the MAPK signaling pathway.

IRS proteins exist in several different isoforms in different tissues and mediate different downstream effects in cells including: glucose uptake in muscle and fat, adipogenesis, hepatic gluconeogenesis and lipogensis, and islet growth and survival (Taniguchi *et al.,* 2006). IRS proteins are activated through tyrosine phosphorylation (via IR), and can be negatively regulated through several mechanisms, including serine phosphorylation in response to insulin, cytokines and other stimuli (Taniguchi *et al.,* 2006). IRS tyrosine phosphorylation activates PI3K through specific tyrosine phosphorylation and is required for insulin action on glucose transport and glycogen synthesis (Taniguchi *et al.,* 2006; Cheatham *et al.,* 1994). Further downstream, PI3K catalyzes the formation of phosphatidylinositol-3,4,5-triphosphate (PIP_3), a intermediary lipid messenger, which activates a number of protein kinases critical for insulin action. The most important downstream effector of PIP_3 is 3-phosphoinosite-dependent protein kinase 1 (PDK1), which can then subsequently contribute to the phosphorylation of Akt/PKB at threonine 308 (Thr308) (Taniguchi *et al.,* 2006).

Akt/PKB is the final critical kinase in the PI3K-Akt/PKB insulin signaling cascade that mediates the phosphorylation of several different downstream substrates. For complete activation it requires phosphorylation at two sites, thr308 as mentioned above, as well as serine 473 (ser473). Akt phosphorylation state can be used as an indicator of insulin stimulation within a tissue, as Akt is considered one of the critical nodes of insulin signaling (Taniguchi *et al.,* 2006).

Akt has been shown to indirectly stimulate glucose transporter 4 (GLUT 4) translocation to the cellular membrane by phosphorylating a mediator protein

called Akt substrate at 160 kDa (AS160), thus promoting glucose uptake from the blood stream and into the cell (Sano *et al.,* 2003). Inhibition of AS160 by phosphorylation allows for re-organization of the cytoskeleton responsible for the translocation of GLUT4 containing vesicles from being sequestered in the cytosol to the plasma membrane (Sano *et al.,* 2003; Cartee & Wojtaszewski, 2007). Akt/PKB activation increased glycogen synthesis through the inhibitory phosphorylation of glycogen synthase kinase -3 (GSK3) (Cross *et al.,* 1995). Additionally, of interest to this project, Akt/PKB has been shown to regulate the expression of gluconeogenic and lipogenic enzymes though the forkhead class of transcription factors. Forkhead box protein O1 (FoxO1) activates gluconeogenic genes such as phosphoenol pyruvate carboxykinase (PEPCK) in liver, and Akt/PKB mediated phosphorylation of FoxO1 attenuates gluconeogenesis (Puigserver *et al.,* 2003).

1.6 Molecular Mechanisms in the AMPK Signaling Cascade

While insulin-mediated regulation of metabolism and storage of glucose and other energy substrates is central to maintaining homeostasis, molecular signaling pathways independent of insulin play an important role in energy balance. One such insulin-independent energy sensor is adenosine monophosphate (AMP)-activated protein kinase (AMPK), which helps regulate cellular metabolism in peripheral tissues such as skeletal muscle, liver, adipose and pancreatic β-cells. Overall, AMPK activation stimulates catabolic pathways, such as glucose uptake and lipid oxidation that produce ATP, while inhibiting anabolic pathways which consume ATP, such as glucose and lipid synthesis (Long & Zeirath, 2006). An elevation in the cellular ratio of adenosine monophosphate to adenosine

triphosphate (AMP:ATP), which is reflective of decreased availability of nutrients in the cell, is the main activator of AMPK. Phosphorylation of the threonine 172 (Thr 172) residue of the α-subunit of AMPK is required for AMPK activity, and is mediated by upstream kinases. The binding of AMP to the γ subunit of AMPK induces a conformational change for allosteric activation and limits the accessibility of phosphatases to the Thr172 binding site, whereas the presence of high levels of ATP suppresses AMPK activation (Hegarty *et al.,* 2009). LKB1 (liver kinase B1) and calmodulin-dependent protein kinase kinase (CaMKK) are two upstream kinases that have been shown to activate AMPK. LKB1, a tumor suppressor, acts constitutively with AMP binding and is the main kinase responsible for AMPK activation in liver, adipose and skeletal muscle tissues (Long & Zeirath, 2006; Hegarty *et al.,* 2009). CaMKK activation of AMPK is triggered by a rise in cellular calcium ions, independent of any changes in the AMP:ATP, but does not appear to contribute significantly to AMPK phosphorylation in the major tissues involved in fuel homeostasis (Hawley *et al.,* 2005; Hegarty *et al.,* 2009).

The action of AMPK in muscle and liver are of significant interest because AMPK is sensitive to cellular levels of ATP and can influence energy metabolism independent of insulin stimulation. AMPK activation is thought to increase glucose transport into skeletal muscle through two main mechanisms: promotion of total gene expression of GLUT 4 and inducing GLUT 4 translocation to the cellular membrane (Hegarty *et al.,* 2009). Conversely, within the liver AMPK activation plays a stronger role in regulating hepatic glucose output, rather than glucose uptake. AMPK has been shown to contribute to suppressed expression of the

gluconeogenic enzymes PEPCK and glucose-6-phosphatase (G6P) through transcriptional regulation (Hegarty *et al.,* 2009).

Additionally, the AMPK pathway has significant effects on lipid metabolism (Long & Zierath, 2006). AMPK reduces malonyl-CoA levels through inhibitory phosphorylation of acetyl-CoA carboxylase (ACC). Malonyl-CoA is a substrate for lipogenesis as well as an inhibitor of lipid oxidation (Hegarty *et al.,* 2009; Saha & Ruderman, 2003). Therefore, it follows that a decrease in cellular malonyl-CoA promotes fatty acid oxidation and inhibits lipid synthesis in skeletal muscle and liver. Chronic AMPK activation has also been shown to reduce expression of hepatic lipogenic genes including ACC (Hegarty *et al.,* 2009; Zhou *et al.,* 2001).

1.7 Glucose Homeostasis in Skeletal Muscle

Alterations in skeletal muscle glucose metabolism are important to assess because skeletal muscle tissue is the major site of insulin-stimulated glucose disposal in the body (DeFronzo *et al.,* 1985). The primary glucose transporter expressed in skeletal muscle is GLUT 4, which is responsible for the majority of glucose uptake into skeletal muscle (Merry & McConnell, 2009; Thai *et al.,* 1998). The translocation of GLUT 4 from intracellular storage vesicles to the plasma membrane is an essential component of extracellular glucose uptake into the cell (Merry & McConnell, 2009). Insulin stimulation rapidly increases glucose transport in skeletal muscle. While the specifics of insulin stimulated glucose transport are complex, simplistically speaking IR activation by insulin on the cell surface initiates activation of the PI3K signaling pathway. The PI3K pathway stimulates GLUT 4

vesicle translocation to the surface of the cellular membrane, resulting in increased glucose uptake into the cell (Taniguchi *et al.,* 2006; Karlsson *et al.,* 2009).

Transcriptional activation of the GLUT 4 gene requires, in addition to other factors, the binding of the transcription factor myocyte enhancer factor 2 (Mef2) to the promoter. It has been demonstrated that insulin stimulation increases both Mef2 binding to the GLUT4 promoter gene as well as the expected increase in GLUT 4 expression (Thai *et al.,* 1998). Interestingly, the development of a muscle-specific insulin receptor knockout mouse showed that despite the ablation of muscle insulin signaling, these transgenic mice were able to maintain relatively normal blood glucose through compensatory mechanisms mediated by exercise and adipose tissue uptake of glucose (Kahn, 2003).

It has been shown that pharmacologically-induced increases in the AMP:ATP ratio in skeletal muscle increases AMPK activation (LeBrasseur *et al.,* 2006). Following this, it is known that acute AMPK activation has been shown to induce increases in GLUT 4 vesicle translocation to the plasma membrane, leading to an increase in glucose uptake into the muscle (Kurth-Kraczek *et al.,* 1999). The increase in AMPK induced GLUT4 vesicle translocation is thought to be mediated through AMPK phosphorylation of AS160, the same intermediate which is phosphorylated by Akt in the insulin-stimulated glucose uptake pathway (Cartee & Wojtaszewski, 2007). As mentioned above, AMPK activation not only increases glucose uptake acutely, but chronic AMPK activation has been shown to increase total expression of GLUT4 (Hegarty *et al.,* 2009). Recently, it was shown that AMPK phosphorylates a histone deacetylase which acts as a suppressor of Mef2 binding to the GLUT 4 gene

promoter in myocytes. Removal of the histone deactylase allows for Mef2 to interact with the GLUT 4 promoter, thus resulting in AMPK-induced increases in total GLUT 4 protein expression (McGee *et al.,* 2008; Hegarty *et al.,* 2009).

Increases in AMPK activation in muscle not only result in an increase in glucose uptake independent of insulin as previously discussed, but also increases insulin sensitivity in muscle (Fisher *et al.,* 2002). This shows that interactions between the AMPK signalling pathway and the insulin signaling pathway can work in combination to enhance muscle glucose homeostasis.

1.8 Glucose Homeostasis in the Liver

As mentioned previously, the liver plays a central role in glucose metabolism and homeostasis. Interactions and regulation of glucose at the liver is influenced by many factors, but the primary regulators of glucose flux in the liver are insulin and glucagon. Insulin acts on the liver in the fed state, or high plasma glucose levels, promoting glucose uptake, glycogen synthesis and suppression of gluconeogenesis. In contrast, glucagon and glucocorticoids act in the low plasma glucose state, fasting, to promote hepatic glucose production through increased glycogenolysis and increased gluconeogenesis (Cherrington, 1999). Hepatic gluconeogenesis is crucial in supplying glucose to tissues throughout the body in prolonged fasting. However, the inappropriate activation of hepatic gluconeogenesis is often seen in diabetes, further exacerbating hyperglycemia (Cherrington, 1999; Puigserver *et al.,* 2003). Insulin-stimulated suppression of hepatic gluconeogenesis acts indirectly to suppress two rate-limiting gluconeogenic enzymes, PEPCK and G6P. PEPCK is responsible for catalyzing conversion of oxaloacetate to phosphoenolpyruvate, the

first committed step in gluconeogenesis. Conversely, G6P is responsible for dephosphorylating glucose-6-phosphate to produce free glucose, the final step in gluconeogenesis as well as glycogenolysis (Yabaluri & Bashyam, 2009).

The transcriptional co-activator peroxisome proliferative activated receptor-γ co-activator 1 (PGC-1α) acts in conjunction with the FoxO1 transcription factor to regulate expression of gluconeogenic enzymes (Puigserver *et al.,* 2003). PGC-1α binds and co-activates FoxO1, which allows for the complex to bind to the promoter region of the PEPCK and G6P genes. Following insulin stimulation, Akt phosphorylates FoxO1 and sequesters it in the nucleus. Akt phosphorylation also interferes with binding the PGC-1α-FoxO1 complex, as well as the complex binding to the gene promoter region, thus inhibiting expression of gluconeogenic proteins (Puigserver *et al.,* 2003; Li *et al.,* 2007). As mentioned previously, insulin stimulation, via Akt phosphorylation, deactivates GSK3, which leads to the activation of glycogen synthase and an increase in glycogenesis (Biddinger & Kahn, 2006).

In order to further understand the contribution of insulin to hepatic glucose regulation, a liver-specific insulin receptor knockout mouse was developed. The mice exhibited hyperglycemia in the fasted and the fed state, and the impaired glucose tolerance appeared to stem from the lack of insulin-induced suppression of hepatic glucose production (Biddinger & Kahn, 2006). Liver specific insulin resistance in these insulin receptor knockout mice is also characterized by the increased expression of the gluconeogenic enzymes PEPCK and G6P (Biddinger & Kahn, 2006).

AMPK, like insulin, plays a role in the regulation of glucose metabolism in the liver (Long & Zierath, 2006). AMPK activation inhibits expression of PEPCK and G6P in liver tissue, leading to suppressed hepatic gluconeogenesis (Hegarty *et al.,* 2009). Koo and colleagues (2005) have demonstrated that AMPK phosphorylation inhibits the action of the transcriptional regulator transducer of regulated cAMP-response element binding protein activity 2 (TORC2) responsible for the expression of PGC-1α, causing PGC-1α to be sequestered in the cytosol, thus limiting its promotion of gluconeogenesis (Long & Zierath, 2006). Consistent with evidence of AMPK-mediated phosphorylation of PCG-1α, deletion of LKB1, an upstream kinase of AMPK, results in the accumulation of TORC2 in the nucleus, resulting in increases in gluconeogenesis (Shaw *et al.,* 2005; Long & Zierath, 2006). However, recent evidence from a model of liver-specific knockout of AMPK showed plasma glucose control, normal glucose production and gluconeogenic gene expression. In this model, inhibition of hepatic glucose production correlated in a dose-dependent manner with reductions in intracellular ATP content, independent of transcriptional regulation and the LKB1/AMPK signaling pathway (Foretz *et al.,* 2010).

1.9 Reactive Oxygen Species and Glucose Metabolism

The role of oxidative stress in the development of diabetes and insulin resistance is complex and not yet fully elucidated. On one hand, it is shown that increased production of reactive oxygen species (ROS) as a result of oxidative stress can impair β-cell function and increase hyperglycemic inflammation (Green *et al.,* 2004). The β-cell does not produce high concentrations of antioxidant enzymes

and is highly susceptible to oxidative damage. Additionally, mitochondrial oxidative phosphorylation is a major source of ROS production within cells which can damage plasma membranes, lipids, proteins and nucleic acids (Green *et al.,* 2004). In muscle, it appears that chronic low-level oxidative stress and acute large increases in ROS may have a deleterious effect on muscle cells, including fatigue (Merry & McConnell, 2009). However, there are studies linking the acute low-level generation of ROS to the initiation of signaling cascades (Merry & McConell, 2009). Toyoda and colleagues (2004) have demonstrated that acute oxidative stress activates AMPK via a mechanism independent of changes in the AMP:ATP ratio. This AMPK activation leads to an increased rate of glucose transport in rat fast-twitch epitrochlearis muscle tissue (Toyoda *et al.,* 2004). Despite this finding, the mechanism by which ROS stimulates glucose uptake remains controversial, as some evidence shows that hydrogen peroxide stimulation increases activation of the PI3K-Akt/PKB insulin signaling pathway (Merry & McConnell, 2009). Hydrogen peroxide incubation of isolated skeletal muscle increases glucose uptake into the muscle. Hydrogen peroxide-induced glucose transport was associated with increased phosphorylation of Akt and decreased with pharmacological inhibition of PI3K. However, in this study, neither ATP levels in the cell nor any changes in AMPK activation were detected (Higaki *et al.,* 2008).

Of interest in this project, Berdanier and Everts (2002) have shown that there is a decreased respiratory control ratio, which is a measure of mitochondrial oxidative function, in BHE/cdb hepatocytes. This decrease in mitochondrial function could contribute to increased ROS production. Additionally, increased markers of oxidative stress and ROS production were found in 43 week-old female BHE/cdb

rat islets and associated with decreased glucose-stimulated insulin secretion (Saleh *et al.,* 2008).

1.10 Lipid Metabolism and Insulin Sensitivity

Abnormal regulation of lipids may contribute to dysfunction and insulin resistance. Insulin resistance can be defined as a condition in which normal concentrations of insulin produce a subnormal biological response. Insulin resistance is common in physiological and pathological states, including obesity and T2D (Taniguchi *et al.,* 2006). The development of whole-body and tissue-specific lipotoxicity-induced insulin resistance has been associated with accumulation of lipids and lipid intermediates, especially diacylglycerol, in insulin-sensitive muscle and liver tissues (Samuel *et al.,* 2010; Hegarty *et al.,* 2009). Peripheral insulin resistance has been associated with increased intramyocellular lipids and decreased oxidative phosphorylation efficiency in muscle. However, the contribution of mitochondrial dysfunction to intramyocellular lipid accumulation in insulin resistance remains debated (Schiff, *et al.,* 2009). Additionally, intrahepatic triglyceride content has been associated with increased insulin resistance and increased triglyceride secretion into the plasma (Samuel *et al.,* 2010). However, prevention of lipid accumulation and increased energy expenditure, such as through increased mitochondrial uncoupling, has been shown to improve insulin sensitivity in some models (Samuel *at al.,* 2010).

Due to the role of AMPK activation in lipid regulation, AMPK-stimulated fatty acid oxidation in liver and muscle tissue would be expected to reduce lipid accumulation, and thus improve insulin action in that tissue (Hegarty *et al.,* 2009).

The regulation of lipid metabolism involves multiple downstream targets, all of which can result in decreased tissue-lipid storage or increased lipid oxidation. Indeed, AMPK-mediated decreases in muscle and liver tissue lipid accumulation have been associated with increased insulin sensitivity (Long & Zierath, 2006).

In the liver, as discussed previously, PGC-1α is an important regulator of glucose homeostasis in the fasting state. In an insulin-resistant state, insulin-stimulated suppression of hepatic gluconeogenesis is reduced, but hepatic lipogenesis is not attenuated, contributing to excess plasma lipid levels in conjunction with hyperglycemia (Li *et al.,* 2007). Interestingly, as a confirmation of this pathogenic mechanism, Li and colleagues (2007) have recently demonstrated that insulin stimulation can directly inhibit PGC-1α through Akt-mediated phosphorylation. PGC-1α phosphorylation prevents its activation of medium-chain acetyl-CoA dehydrogenase, which is an activator of lipid β-oxidation. Thus, insulin stimulation results in a decrease in lipid oxidation (Li *et al.,* 2007). It should be noted that there has been some evidence that reduced ATP availability in the hepatocyte following caloric restriction was associated with enhanced PI3K-Akt mediated insulin signaling, but a similar effect was not seen in muscle (Barazzoni *et al.,* 2005). Conversely, caloric restriction induced increases in lean tissue oxidative capacity associated with reduced tissue triglyceride content in muscle, but not in liver tissue, suggesting a pathway for an adaptive response (Barazzoni *et al.,* 2005).

In a similar manner to insulin, AMPK activation in the liver contributes to hepatic lipid regulation. Glucose-induced expression of genes associated with lipid synthesis such fatty acid synthase and ACC is suppressed by AMPK activation

(Long & Zierath, 2006). As mentioned above, pharmacological activation of AMPK increases fatty acid oxidation through inhibition of ACC contributing to decreased intracellular lipid deposition in liver, which can contribute to an increase in tissue insulin sensitivity (Zhou *et al.,* 2001). In addition to the promotion of insulin sensitivity, mechanisms promoting lipid oxidation and prevention of intrahepatic lipid accumulation are of particular interest in this project as the BHE/cdb rat has been shown to have a fatty liver, which is worsened with high fat and high-sugar diets (Berdanier, 2007).

2.0 Study Rationale

2.1 Rationale

Previous studies by Berdanier and colleagues have shown that BHE/cdb rats develop impaired glucose tolerance with age (Berdanier, 2007). However, while female BHE/cdb rats in our lab have developed impaired glucose tolerance with age, the male BHE/cdb rats did not develop impaired glucose tolerance up to 1 year of age (Saleh et al, 2008). In fact, previous work in our lab has shown that at 21 weeks of age, male BHE/cdb rats actually demonstrate enhanced glucose tolerance, but the mechanism was not reported (Chan, unpublished data). It has been demonstrated that diet and environmental factors can impact the progression and severity of impaired glucose tolerance in the BHE/cdb model of mitochondrial diabetes (Berdanier, 2007; Everts & Berdanier, 2002; other Mathews *et al.,* 2000). However, the specific molecular mechanisms associated with enhancements in peripheral glucose homeostasis in the BHE/cdb model have not been well documented. A reduction in the efficiency of mitochondrial respiration was reported in the liver of BHE/cdb rats (Everts & Berdanier, 2002). Female BHE/cdb rats at 43 weeks of age have been shown to have increased markers of oxidative stress in pancreatic β-cells, indicating that there is increased ROS production (Saleh *et al.,* 2008). Additionally, in the same female BHE/cdb rats, AMPK phosphorylation and ACC phosphorylation is increased relative to controls in pancreatic islets as well as decreased ATP synthesis in response to glucose stimulation (Saleh *et al.,* 2008).

Therefore, in combining the knowledge that low cellular ATP levels and oxidative stress have been shown to activate AMPK, enhanced AMPK signaling in peripheral

tissues in the male BHE/cdb rat may contribute to the observed enhanced glucose tolerance at 21 weeks (LeBrasseur *et al.,* 2006; Toyodo *et al.,* 2004). Additionally, following observations that intracellular lipid in liver and muscle could contribute to peripheral insulin resistance, enhanced lipid oxidation as a result of AMPK activation may contribute to increases in insulin sensitivity as BHE/cdb rats are reported to have fatty livers (Samuel *et al.,* 2010; Berdanier, 2007). Additionally, some evidence suggests that preferential activation of the insulin signaling pathway may occur as a result of a compensatory mechanism as a result of decreased insulin production, or decreased cellular availability of ATP (Maassen *et al,* 2004; Fisher *et al.,* 2002).

2.2 Research Objectives

Determine whole body and molecular mechanisms which could contribute to enhanced glucose tolerance in 21 week-old male BHE/cdb rats. The relationship between reduced cellular ATP and enhanced glucose tolerance will be explored by investigating whether there are:

i. Differences in whole body *in vivo* metabolism, including glucose and lipids.

ii. Changes in whole body composition or liver and muscle tissue specific composition and lipid accumulation.

iii. Increases in activation of the insulin-independent AMPK signaling pathway in liver and skeletal muscle.

iv. Increased or preferential activations in the PI3K-Akt insulin signaling pathways in muscle and liver.

2.3 Research Hypothesis

Low cellular ATP as a result of the genetic mutation in the BHE/cdb rat enhances peripheral glucose tolerance through increased AMPK activation, resulting in: i) increased fat oxidation; ii) increased insulin sensitivity; and iii) increased glucose transporter expression.

3.0 Materials and Methods

3.1 Treatment of Animals

All procedures involving animals were approved by the Animal Care and Use Committee of the University of Alberta and were in accordance with the guidelines of the Canadian Council on Animal Care and the National Institutes of Health (NIH) Principles of Laboratory Animal Care. Breeding pairs of BHE/cdb rats were obtained from NIH (Bethesda, MD, USA). Genotyping to confirm the mitochondrial mutation in the BHE/cdb strain was done as previously described (Mathews *et al.*, 1995). Offspring were weaned at three weeks of age onto a standard chow diet, unless otherwise indicated. Strain-matched controls without the mitochondrial mutation were no longer available. Therefore, as has been done previously, Sprague-Dawley rats were used as controls (Saleh *et al.,* 2008; Mathews *et al.,* 1995; Mathews *et al.,* 1999). Age-matched Sprague Dawley (SD) rats were purchased from Charles River Canada (St Constant, QC) or the Department of Biology, University of Alberta. Male rats were raised to 21 weeks of age under standard housing conditions with a 12 hour light-dark cycle. Additionally, at 17 weeks of age a small group of both BHE/cdb and SD rats were placed on a high fat diet (HFD) for 4 weeks prior to procedures. The HFD consisted of composed of 20% w/w fat compared to 5% w/w in the standard chow diet (Table 3.1). The composition of the HFD, which consisted of mostly saturated fat, was matched to the commercially available chow diet (5001 Laboratory Rodent Diet, LabDiet, PMI Nutrition International, St. Louis, MO, USA), with the proportion of carbohydrates in the HFD reduced to accommodate for the increased fat content. Food was withdrawn approximately 16 hours prior to procedures requiring overnight fasting.

Table 3.1- Rodent Diet Composition

Ingredient (g)	High Fat Diet (HFD)
Casein	270
L-Methionine	2.5
Dextrose	189
Corn Starch	169
Cellulose	100
Essential Nutrients & Minerals	70.1
Canola Sterine	99.5
Flaxseed Oil	6
Sunflower Oil	94.5
Total Weight	1079.6

3.2 Measurement of Whole-Body *In Vivo* Metabolic Parameters

The Oxy-Max comprehensive lab animal monitoring system (CLAMS) (Columbus Instruments, Columbus, OH, USA) was used to measured oxygen consumption (VO_2), carbon dioxide production (VCO_2), respiratory exchange ratio (RER), heat production (kcal/hr), food consumption, water consumption and total activity counts. Animals were housed individually then underwent an acclimatization period of approximately 21 hours, followed by a data collection period of approximately 29 hours. Data over a 24 hour period was analyzed, consisting of a 12 hour light cycle and a 12 hour dark cycle. Ground chow and water were available *ad libitum* and were measured for mass and volume consumed over time, respectively. RER was calculated as a ratio of carbon dioxide production to oxygen consumption (equation 3.1a). Heat production was calculated from a derived internal calorific value based on the observed RER and the VCO_2 (equation 3.1b)

then corrected for body mass to yield kcal/hr/kg (equation 3.1c) (McLean & Tobin, 1987).

Equation 3.1: *a. $RER = (VCO_2)/(VO_2)$*

b. $CV = (3.815+1.232) \times RER$

c. $Heat = (CV \times VO_2)/mass$

Activity was measured using a photocell based activity monitor and reported as total activity counts in the x, y & z axis over the monitoring period. Magnetic resonance imaging (MRI) was used to determine fat and lean mass body composition using the EchoMRI Whole Body Composition Analyzer (Echo Medical Systems LLC, Houston, TX, USA).

3.3 Glucose, Insulin, and Pyruvate Tolerance Tests.

Intraperitoneal (ip.) glucose tolerance tests (ipGTT), insulin tolerance tests (ITT) and pyruvate tolerance tests (PTT) were performed at 21 weeks of age following an overnight fast. Briefly, for ipGTTs, baseline (t=0) blood samples were collected from a clipped tail vein followed by an ip. injection of 1.0 g/kg of glucose in sterile saline. Blood samples from the tail vein were collected at t=10, 20, 30, 60, 90 & 120 minutes. Blood glucose was determined using a glucometer (Accu-Chek Compact Plus, Roche Diagnostics, Laval, QC) on fresh samples. Blood for plasma samples was collected in heparin-coated glass capillary tubes, centrifuged and plasma samples were collected and frozen at -80°C until use. Plasma insulin concentration was determined by enzyme-linked immunosorbent assay (ELISA) (Alpco Diagnostics, Salem, NH, USA) as per manufacturer's directions using a spectrophometric microplate reader (Molecular Devices, Sunnyvale, CA, USA). During ITTs, animals received an ip. injection of 20 µg/kg dose of 1mg/mL insulin

in sterile saline with blood glucose determination at t=0, 15, 30, 60, 90 & 120 minutes. PTTs involved ip. injection of 2mg/kg sodium pyruvate in sterile saline followed by blood glucose determination as per ipGTT method.

3.4 Tissue Collection

Rats were anesthetized using ip. injection of xylazine (7 mg/kg) and ketamine (75 mg/kg). Tissues were collected in the fed and fasted state. In the fasted state, one half of the animals received an ip. injection of 1.0 mg/kg insulin in saline, or equivalent volume of saline, 10 minutes prior to euthanasia. Liver, soleus muscle and epitrochlearis muscle tissues were excised and immediately frozen in liquid N_2. Samples were stored at -80°C until use.

3.5 Immunoblotting

Tissues were homogenized in lysis buffer (12µL buffer/µg of tissue) (Kim *et al.*, 2004) and stored at -80°C until use. Immunoblotting was performed following SDS-PAGE and electrophoretic transfer under standard conditions. Protein concentration of homogenized samples was determined using a colourimetric assay in triplicate using the bicinchoninic acid assay (BCA) method (Smith *et al.,* 1985). Samples were prepared to a standard protein concentration of 2.0 µg/µL in Laemmli Sample Buffer and heated at 95°C for 5 minutes before separation. Proteins were separated using 10% polyacrylamide gels and transferred onto nitrocellulose membranes for approximately 90-120 minutes at 200 mA per tank using wet electrophoresis. Membranes were blocked for 1 hour in 5% (w/v) non-fat dry milk diluted in tris-buffered (pH 7.4) saline-0.1% Tween 20 (TBST-5% milk) with gentle agitation. Membranes were incubated overnight at 4°C in either TBST-5% milk or TBST-5% Bovine Serum Albumin (BSA) (w/v) with the

appropriate primary antibodies (see Table 3.2). After brief washing, membranes were probed with appropriate secondary antibodies (1:5000) in TBST-1% (w/v) milk for 1 hour. Protein bands were visualized using a Typhoon Imaging System (GE Healthcare, Mississauga, ON) following development with ECL Plus (GE Healthcare). Band intensity of protein of interest was determined relative to intensity of control protein using ImageJ software (U.S. National Institutes of Health, Bethesda, MA, USA). Protein expression was shown relative to β-actin in liver and relative to α-actin, α-tubulin, or GAPDH in muscle, depending on the size of the protein of interest.

Table 3.2 – Antibody Sources and Dilutions

Antibody	Source	Catalog Number	Dilution
Phospho-ACC	Cell Signaling, Danvers, USA	#3361	1:1000
α- actin	Sigma, Mississauga, ON	Unknown	1:10000
β-actin	Sigma	#A5441	1:5000
Phospho-Ser473-Akt	Cell Signaling	#4060	1:1000
Phospho-Thr308-Akt	Cell Signaling	#9275	1:2000
Phospho-Thr172-AMPK	Cell Signaling	#2531	1:1000
Catalase	Sigma	#C0979	1:4000
GAPDH	Santa Cruz Biotechnology, Santa Cruz, CA, USA	#sc-47724	1:1000
GLUT4	Cell Signaling	#2213	1:2000
Mn-SOD	Enzo Life Sciences, Ann Arbor, MI, USA	#SOD111	1:2000
PEPCK	Cayman Chemicals, Ann Arbor, MI, USA	#10004943	1:2000
α-tubulin	Sigma	#T6199	1:1000

3.6 Glycogen Determination

A colourimetric assay was used to determine tissue glycogen content after extraction (ab65620, Abcam, Cambridge, UK). Tissue (10mg/200µL dH_2O) was homogenized on ice with a benchtop homogenizer (FastPrep 24, MP Biomedicals LLC., Solon, OH, USA) and 1.0 mm glass beads (Bio Spec Products Inc., Bartlesville, OK, USA). As per the kit manufacturer's instructions, glycogen was hydrolyzed to glucose, which was then oxidized to generate a product that reacts with a colour probe, which was then quantified by spectrophotometery using a microplate reader at 570 nm (Molecular Devices).

3.7 Tissue Lipid Determination

Total lipid analysis of liver and soleus tissue was conducted using gas-liquid chromatography (GC). Following homogenization of frozen tissue samples and standardization of protein content in lysis buffer (1mg/mL), phospholipids in the samples were digested using phospholipase-C (2mL enzyme solution(17.5mM Tris, 10 mM $CaCl_2$, pH7.3, 2 units PL-C)/mg protein; Sigma, Mississauga, ON) and diethyl ether in vortex for 2 hr at 30°C to remove polar head groups. Lipids were prepared with tridecanoin as an internal standard and extracted using 2:1 cholorform:methanol, with the lower phase removed by passing through a Pasteur pipette containing anhydrous Na_2SO_4. Samples were then evaporated under N_2, followed by incubation in Sylon BFT (Supelco Analytical, Bellefonte, PA, USA) for 1 hr, evaporated, and re-dissolved in hexane. Samples were run in a Zebron ZB-5 column (Phenomenex Inc., Torrance, CA, USA) using an HP Agilent 6890 GC Gas Chromatograph with flame-ionization detector (Agilent, Mississauga, ON). Area

under the curve was used to assess lipid peaks, and concentration was expressed relative to tridecanoin internal standard.

3.8 Transcription Factor Activation

Nuclear extracts were prepared from previously frozen tissues using a kit (Active Motif, Carlsbad, USA). Tissue samples were homogenized on ice in hypotonic buffer with 1M dithiothreitol (DTT) and protease inhibitors. Following homogenization, tissues were incubated in lysis buffer (3mL/g tissue) and then centrifuged to collect nuclear fraction. Nuclear translocation of the transcription factors myocyte enhancer factor 2A (Mef2A) and forkhead box protein O1 (FoxO1) were measured using Trans-AM kits measuring binding to specific DNA consensus sequences according to the manufacturer's instructions (Active Motif). Briefly, this consisted of oligonucleotide coated plates to which cell extract containing activated transcription factor was added, followed by 1 hr incubations with primary antibody and anti-IgG HRP (horse radish peroxidase) conjugate. After addition of a colourimetric developing solution and stop solution, the plate was read using spectrophotometry at 450nm with a reference wavelength of 655nm (Molecular Devices).

3.9 Statistical Analysis

All data are expressed as mean ± standard error (SE), and in all cases $p < 0.05$ was considered statistically significant. Student's t-test or two-way ANOVA followed by multiple Bonferroni comparisons were conducted as appropriate in order to determine statistical significance using GraphPad Prism 5 (GraphPad Software Inc, La Jolla, CA, USA). Area under the curve (AUC) was calculated using the trapezoidal method, where C is the glucose or insulin concentration at the various time points,

t_n (Equation 3.2). The product of the insulin area under the curve and glucose area under the curve of the ipGTT was calculated, as this value can be used as a marker of systemic insulin action (Sutherland *et al.,* 2008).

Equation 3.2 – $AUC = \sum ½ (C_{(n+1)} + C_n) \times (t_{(n+1)} - t_n)$

Table 3.3 - Materials

Name	Source	Catalog Number
Acrylamide /Bis (37.5:1)	BioRad, Mississauga, ON	161-0159
Ammonium Persulfate (APS)	Amresco, Solon, OH, USA	UN1444
Aprotonin	Sigma	A6729
Bicinchoninic Acid Solution (BCA)	Sigma	B9643
Bovine Serum Albumin (BSA)	Santa Cruz Biotechnology	Sc-2323
Bromophenol Blue	BioRad	161-040
Chloroform	Fisher Scientific	C298-4
Copper (II) Sulphate	Sigma	C2284
DTT (dithiothreitol)	Active Motif, Carlsbad, CA, USA	100602
ECL+	GE Healthcare, UK	RPN2132
EDTA (Ethylene-diaminetetraacetic acid)	BDH Chemicals, Toronto, ON	B10093
Glycine	Fisher Scientific	BP381-1
Glycogen Assay Kit	Abcam	Ab65620
HCl (hydrochloric acid)	Fisher Scientific	UN1789
Hexanes	Fisher Scientific	H302-4
Insulin (human)	Sigma	I2643
Insulin ELISA	Alpco Diagnostics	80-INSRT-E10
Ketamine HCl (Vetalar)	Bioniche Animal Health Canada Inc., Belleville, ON	01989529
KCl (Potassium Chloride)	Sigma	P9333
Leupeptin	Sigma	L2884
Methanol (MeOH)	Fisher Scientific	A412P-4
NaCl (Sodium Chloride)	Fisher Scientific	BP358-212
NaOH (Sodium Hydroxide)	Fisher Scientific	S318-500
Nuclear Extraction Kit	Active Motif	40010
Phospholipase-C (PL-C)	Sigma	P7633-125UN

Name	Source	Catalogue No.
PMSF (Phenylmethane-sulfonylfluoride)	Sigma	P7626
Precision Plus Protein Standards- Dual Colour	BioRad	161-0374
SDS (Sodium dodecyl sulfate)	Sigma	L6026
SMP (skim milk powder)	Saputo, Montreal, QC	n/a
Sodium deoxycholate	Gibco, Grand Island, NY, USA	D6750
Sodium pyruvate	Sigma	P2256
Sodium sulphate (anhydrous)	Sigma	239313
Sodium orthovanadate	Sigma	S6508
Sylon BFT (BSTFA +TMSC, 99:1)	Supelco Analytical, Bellefonte, PA, USA	3-3148
TEMED	Gibco BRL, Gaithersburg,MD, USA	5524UB
TransAM FKHR transcription factor assay	Active Motif	46396
TransAM MEF2 transcription factor assay	Active Motif	43196
Tris Base	Boerhringer Mannheim, Indianapolis, IN, USA	604205
Triton X-100	Sigma	x-100
Tween-20	Fisher	BP337-500
Xylazine (Xylamax)	M.T.C. Pharmaceuticals, Cambridge, ON	00805475

4.0 Results

4.1 Whole Body Profile

Body weight was measured at 21 weeks and compared between genotype (BHE/cdb vs. Sprague Dawley as well as standard chow diet and 4 weeks high fat diet (HFD) (Figure 4.1). Overall, SD rats had a significantly larger body weight as compared to BHE/cdb rats, regardless of diet ($p<0.001$) but HFD did not increase overall body weight as compared to chow. There was a significant interaction effect ($p=0.026$), which may be accounted for in that, unexpectedly, BHE/cdb rats on chow diet weighed more than BHE/cdb rats on HFD (BHE/cdb Chow: 473.2 ± 11.5 g; HFD: 459.5 ± 13.2 g; $p> 0.05$), while SD rats on HFD weighed more than on chow (SD chow: 648.0 ± 17.3 g; HFD 717.5 ± 22.2 g). Magnetic resonance imaging was used to assess whole body relative fat and lean mass composition in BHE/cdb and SD rats on standard chow diet (Figure 4.2). However, there was no difference in whole body composition in lean or fat mass.

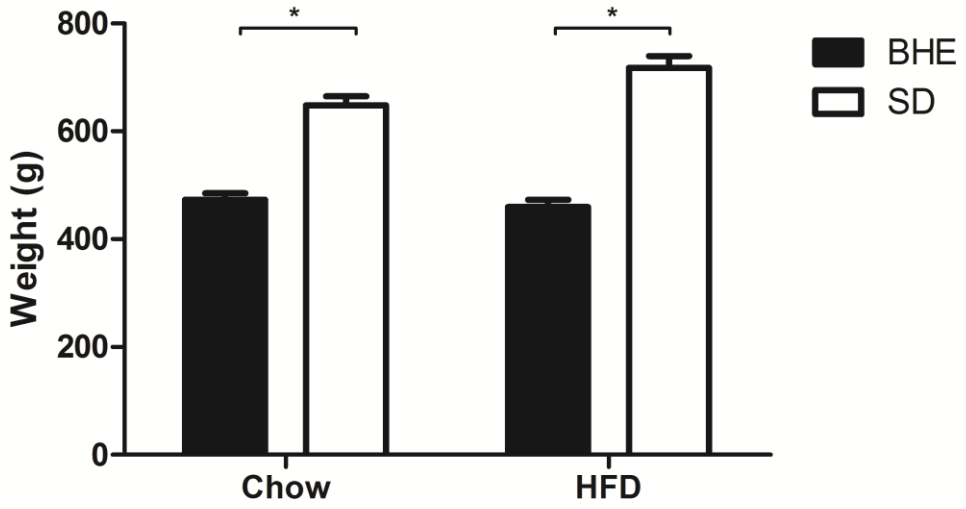

Figure 4.1 – Body weight in 21-week-old rats. Weight of rats on standard chow (n=6) and high fat diet (HFD) (n=8) and compared using 2-way ANOVA. Overall, SD rats were higher in body weight than BHE ($p<0.001$). However, the effect of diet was not significant ($p=0.12$).

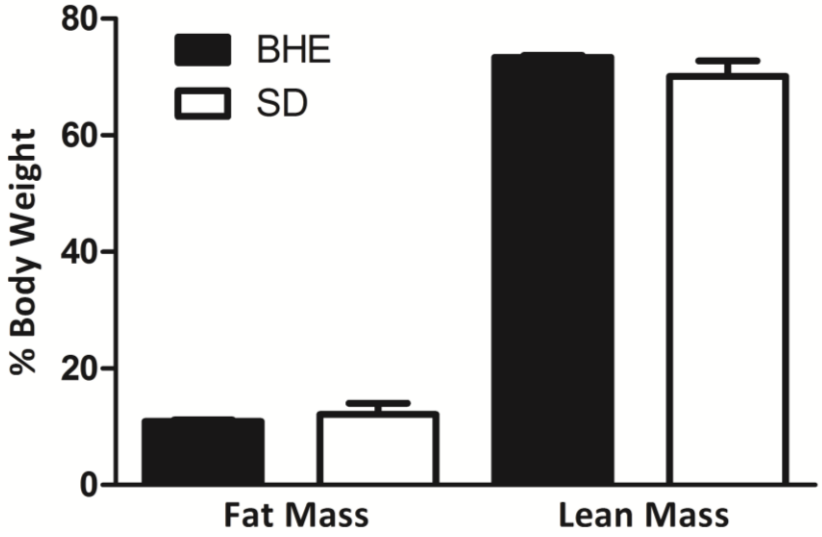

Figure 4.2 – MRI analysis of body composition relative to body weight (n=6). There was no difference between BHE/cdb and SD rats on chow diet in lean mass (p=0.53) or fat mass (p=0.26).

Whole body *in vivo* calorimetry, activity, food, and water consumption was measured over 24 hours using a comprehensive lab animal monitoring system (CLAMS) with the rats maintained on standard chow diet (Table 4.1). CLAMS data were assessed over the whole 24-h study period, as well as during the light and dark cycles. In all parameters measured, values were significantly higher during the dark cycle, as compared to the light cycle (p-values not reported) which is reflective of the normal habits of nocturnal rodents. RER, a ratio which corresponds to the source of energy used in oxidation, was significantly higher in BHE/cdb rats (Figure 4.3A). Similarly, whole body metabolic rate was significantly higher in BHE/cdb as compared to SD rats, as seen in oxygen consumption (Figure 4.3B), carbon dioxide production (Figure 4.3C), and heat production (Figure 4.3D). However, despite differences in whole body metabolism, there was no difference in total activity (Figure 4.4A), food consumption (Figure 4.4B), or water consumption (Figure 4.4C).

Table 4.1 - Comprehensive Lab Animal Monitoring Study Mean Numerical Data

A. Mean RER	24 Hours	Light Cycle	Dark Cycle
BHE/cdb	**0.89** ± 0.02	**0.87** ± 0.02	**0.90** ± 0.01
Sprague Dawley	**0.86** ± 0.02	**0.85** ± 0.02	**0.87** ± 0.01
p value	< 0.01	<0.05	<0.01
B. Mean V O2 (mL/kg/hr)	**24 Hours**	**Light Cycle**	**Dark Cycle**
BHE/cdb	**1148** ± 14	**1089** ± 20	**1208** ± 18
Sprague Dawley	**973.3** ± 9.9	**929.0** ± 14	**1018** ± 11
p value	< 0.01	< 0.01	< 0.01
C. Mean VCO2 (mL/kg/hr)	**24 Hours**	**Light Cycle**	**Dark Cycle**
BHE/cdb	**1018** ± 13	**951.3** ± 17	**1085** ± 17
Sprague Dawley	**839.7** ± 9.0	**791.9** ± 12	**887.5** ± 9.8
p value	< 0.01	< 0.01	< 0.01
D. Heat (kcal/hr/kg)	**24 Hours**	**Light Cycle**	**Dark Cycle**
BHE/cdb	**5.87** ± 0.08	**5.46** ± 0.10	**6.28** ± 0.09
Sprague Dawley	**4.82** ± 0.05	**4.56** ± 0.07	**5.08** ± 0.06
p value	< 0.01	< 0.01	< 0.01
E. Activity (counts)	**24 Hours**	**Light Cycle**	**Dark Cycle**
BHE/cdb	12376 ± 1037	4620 ± 399	7757 ± 824
Sprague Dawley	10998 ± 779	4566 ± 526	6432 ± 449
p value	> 0.05	> 0.05	> 0.05
F. Food Consumption (g)	**24 Hours**	**Light Cycle**	**Dark Cycle**
BHE/cdb	23.2 ± 2.5	7.8 ± 1.9	15.2 ± 1.6
Sprague Dawley	26.8 ± 3.3	11.7 ± 1.7	15.1 ± 2.0
p value	> 0.05	> 0.05	> 0.05
G. Water Consumption (mL)	**24 Hours**	**Light Cycle**	**Dark Cycle**
BHE/cdb	25.3 ± 1.8	6.4 ± 1.0	18.6 ± 1.7
Sprague Dawley	27.0 ± 4.8	10.6 ± 2.2	16.1 ± 4.4
p value	> 0.05	> 0.05	> 0.05

Summary of CLAMS values. (A-D) BHE n=5, SD n=6, (E-G) n=6 for all groups. All data are presented mean ± SEM, with significant values shown in **bold** ($p<0.05$) for BHE rats compared to SD groups.

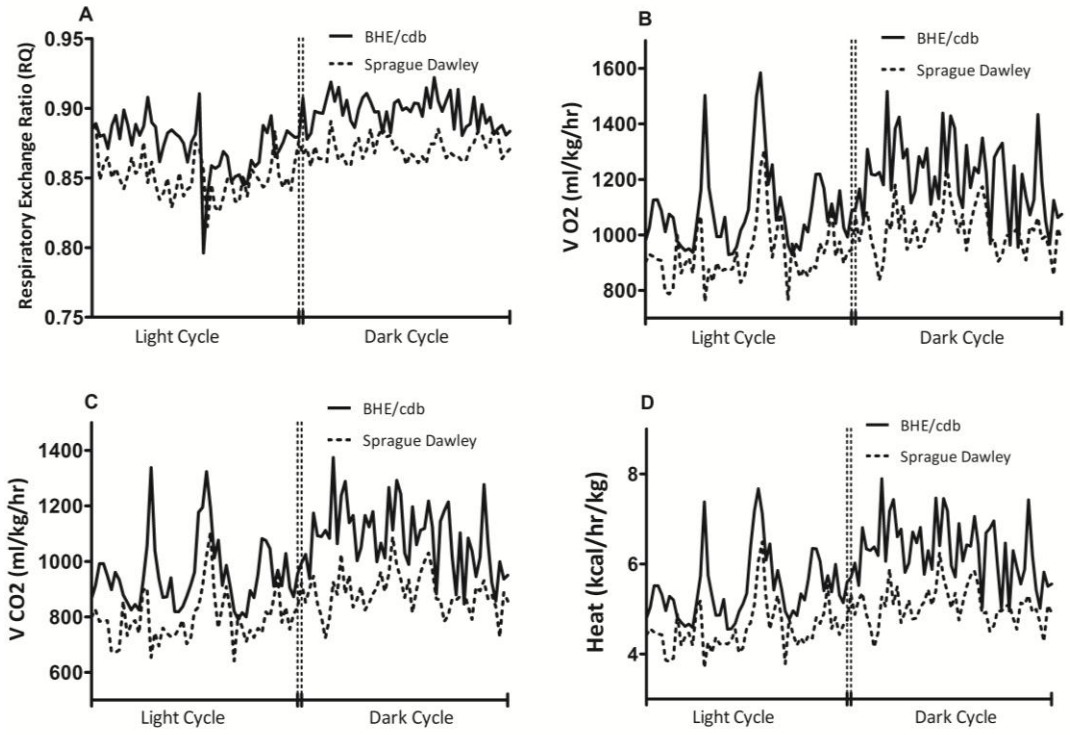

Figure 4.3 – Whole body calorimetry assessed using CLAMS for BHE/cdb (n=5) and SD rats (n=6). (A) Respiratory exchange ratio (RER) (VCO_2/VO_2); BHE/cdb rats have a significantly higher RER, thus preferentially oxidize carbohydrates. (B) Volume of oxygen consumed (VO_2) expressed relative to body weight (mL/kg/hr); BHE/cdb rats have a significantly higher VO_2 than SD rats. (C) Volume of carbon dioxide consumed (VCO_2) expressed relative to body weight (mL/kg/hr); BHE/cdb rats have a significantly higher VCO_2 than SD rats. (D) Whole body heat production, expressed relative to body weight (kcal/hr/kg); BHE/cdb rats generated significantly more heat than SD rats.

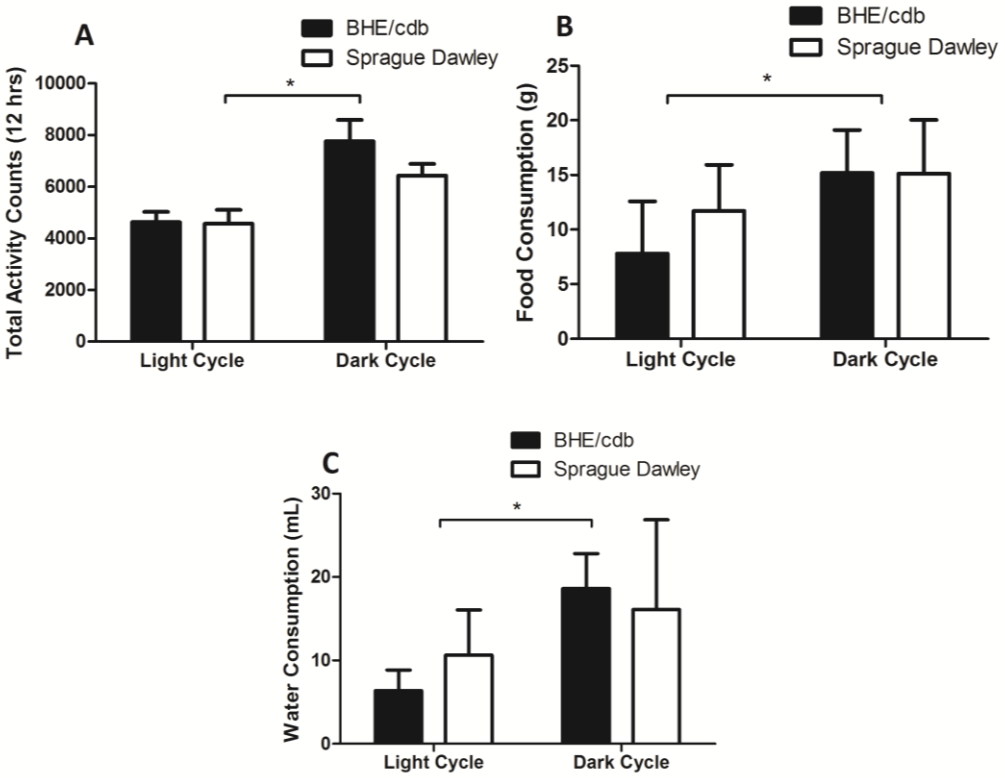

Figure 4.4- CLAMS activity, food & water consumption. No significant differences were seen between BHE/cdb rats or SD rats in (A) total activity counts, (B) cumulative food consumption, or (C) cumulative water consumption. Each of these parameters were significantly higher ($p<0.01$) during the dark cycle than during the light cycle.

4.2 Glucose, Insulin and Pyruvate Tolerance Tests

Intraperitoneal glucose tolerance tests showed enhanced glucose tolerance in the BHE/cdb as compared to SD rats on both standard chow and high fat diets (Figure 4.5). Overall, there was a significant combined effect of diet and genotype on blood glucose levels ($p<0.001$) during the course of the ipGTT as well as a significant interaction effect ($p<0.001$) which may be attributed to the time differences in peak blood glucose concentrations (Figure 4.5A). Post-test analysis showed that on standard chow diet, blood glucose levels are lower in BHE/cdb rats as compared to SD rats at t_{10} and t_{20} (# $p<0.001$). However, BHE/cdb rats on HFD have significantly

higher blood glucose concentrations compared to BHE/cdb chow at t_{10}, t_{20} & t_{30} (*$p<0.01$), and there are no differences between BHE/cdb HFD and the SD chow or SD HFD groups. Glucose AUC analysis shows no overall effect of genotype ($p=0.16$), while AUC HFD is higher than AUC chow, giving a significant overall effect of diet (# $p<0.05$) (Figure 4.5B). However, in the standard chow diet, AUC glucose of BHE/cdb rats is lower than AUC of SD rats (* $p< 0.01$). Additionally there was a significant interaction effect ($p <0.01$), which may be attributed to the fact that, while not statistically significant, AUC of BHE/cdb glucose on HFD is higher than AUC glucose of SD HFD group, which is opposite of the difference seen in the chow diet.

Plasma insulin measurements during the ipGTT showed a significant combined effect of genotype and diet ($p<0.001$), as well as a significant interaction effect (Figure 4.5C). Insulin secretion over the course of the test in BHE/cdb rats was significantly blunted as compared to SD rats when on standard chow diet (*$p<0.001$, t_{10} & t_{20}). While the SD HFD group had significantly higher insulin secretion compared to the SD chow group (# $p<0.01$, t_{10}, t_{20}, t_{30}, t_{60}, t_{90} & t_{120}), there was no change in insulin secretion in the BHE/cdb HFD group when compared to the BHE/cdb chow group. Therefore it follows that BHE/cdb HFD insulin secretion is decreased compared to SD HFD (ϕ $p<0.001$, t_{10}, t_{20}, t_{30}, t_{60}, t_{90} & t_{120}). AUC (Figure 4.5 D) confirms blunted insulin secretion in BHE/cdb rats compared to SD rats in both chow and HFD groups. Overall, glucose tolerance tests conducted show that BHE/cdb rats have enhanced glucose tolerance compared to SD rats despite blunted insulin secretion on a standard chow diet. However, the lower glycemic excursion seen in the BHE/cdb chow group was not maintained when the rats were subjected to the stress of the high fat diet, because the BHE/cdb rats were not

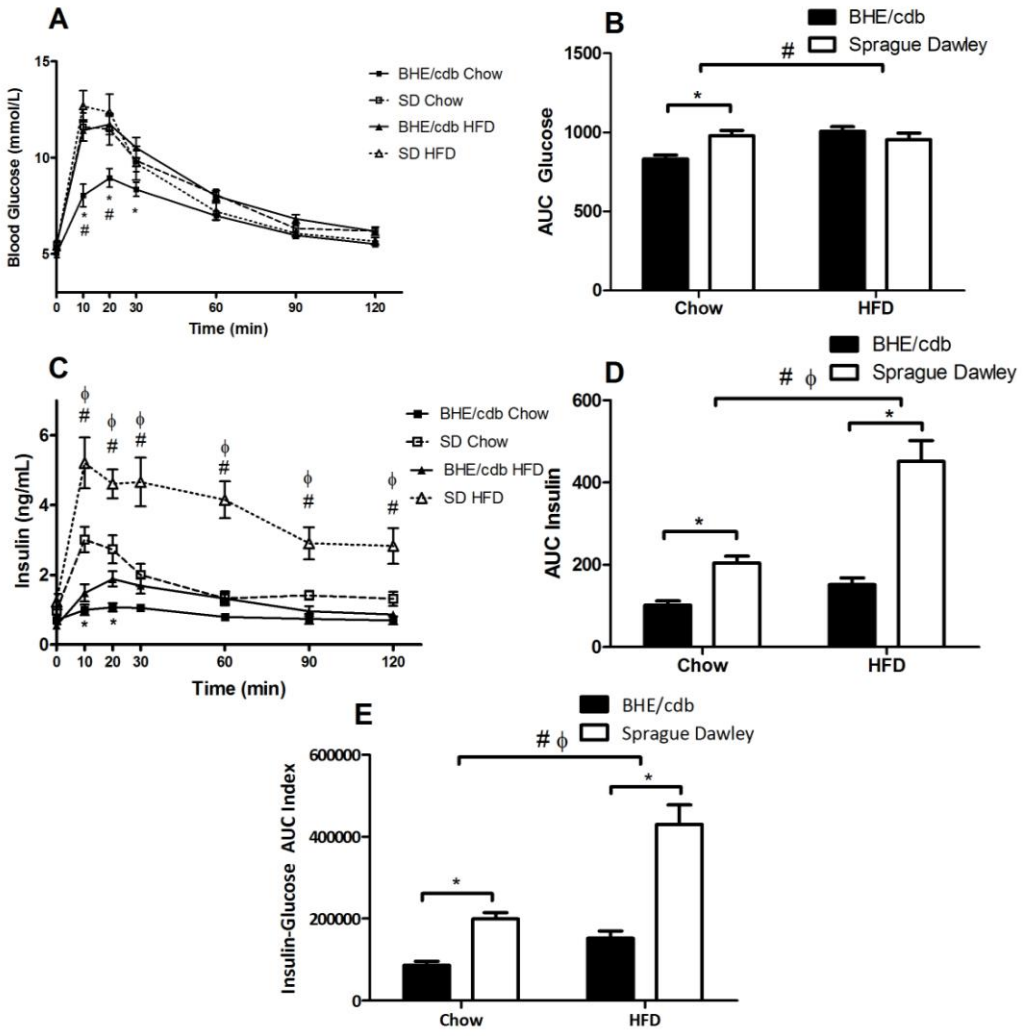

Figure 4.5- Intraperitoneal glucose tolerance tests (1g/kg glucose) analyzed with 2-way ANOVA and Bonferroni's post-tests. (A) Blood glucose values (mmol/L) over the course of the experiment: BHE/cdb glucose is lower than SD rats on chow (#p<0.001), and BHE/cdb glucose is lower in chow groups compared to BHE/cdb HFD (*p<0.01), while there is no difference between BHE/cdb and SD on HFD. (B) Area under the curve glucose values: Significant overall diet effect (#p< 0.05) and SD glucose is larger than BHE/cdb glucose on chow diet (*p<0.01), but not HFD. (C) Plasma insulin values (ng/mL) over the course of the experiment: BHE/cdb chow has decreased insulin secretion compared to SD chow (*p<0.01), but not compared to BHE/cdb HFD. SD HFD insulin secretion is greater than SD chow (#p<0.01) and BHE/cdb HFD (ϕ p<0.001). (D) Area under the curve insulin values: Significant overall effect of diet (# p<0.001) and genotype (p<0.001). SD rats had greater insulin secretion on chow diet (*p<0.01) and HFD (*p<0.001). (E)Integrated insulin-glucose AUC Index: Significant overall effect of diet (#p<0.0001) and genotype (ϕ p<0.001). BHE/cdb rats have better whole body insulin sensitivity on both chow and HFD (* p<0.01).

able to increase insulin secretion sufficiently to maintain lower blood glucose levels. An approximate measure of whole body insulin sensitivity was calculated by multiplying the AUC glucose of each rat with its respective AUC insulin, where a lower product indicates better insulin sensitivity (Sutherland *et al.,* 2008). The resulting integrated insulin-glucose AUC index demonstrated that BHE/cdb rats maintain enhanced insulin sensitivity as compared to SD controls during both chow and HFD feeding (Figure 4.5 E). However, HFD did worsen indications of insulin sensitivity.

Insulin tolerance tests were conducted to assess whole body insulin sensitivity and glucose clearance in chow-fed rats. Glucose clearance from the blood was measured following intraperitoneal injections of insulin (Figure 4.6). Glucose clearance was higher in BHE/cdb rats than SD rats ($p<0.05$, Figure 4.6A). Additionally, area under the curve (Figure 4.6B) for relative glucose was significantly lower in BHE/cdb rats than SD control rats ($p<0.05$). Overall, there

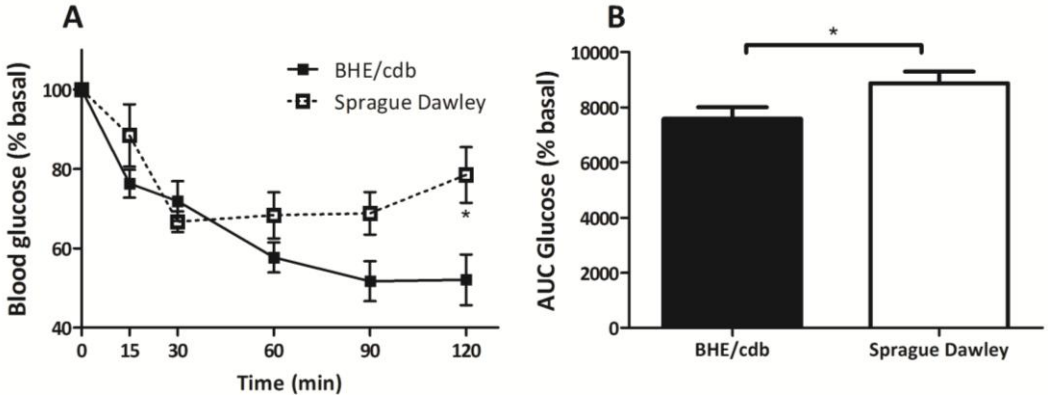

Figure 4.6- Insulin tolerance tests in chow-fed rats. BHE/cdb n=10, SD n=9. (A) Blood glucose relative to baseline. SD rats show overall decreased glucose clearance compared to BHE/cdb ($p<0.05$, 2-way ANOVA), which is significant at t_{120} (*$p<0.01$). (B) Relative glucose area under the curve is decreased in BHE/cdb rats (*$p<0.05$).

was increased glucose disappearance in BHE/cdb rats during the ITT compared to age-matched SD control rats, and the insulin sensitivity index in the ipGTT showed enhanced insulin sensitivity in the BHE/cdb rats. Taken together, these results may indicate increased insulin sensitivity in the BHE/cdb rats.

Finally, pyruvate tolerance tests were conducted in chow-fed rats to assess liver gluconeogenesis. Pyruvate is a substrate used in *de novo* glucose synthesis in the liver, and measurement of glucose following an intraperitoneal injection of pyruvate can be used as a measure of functional gluconeogenesis (Fukushima *et. al.*, 2010). In the PTT, overall blood glucose levels in the BHE/cdb group are lower than the SD group ($p<0.01$, Figure 4.7A), despite no significant difference in net glucose AUC ($p=0.074$, Figure 4.7B). The slightly lower blood glucose seen in the BHE/cdb rats indicates blunted liver gluconeogenesis in response to pyruvate administration.

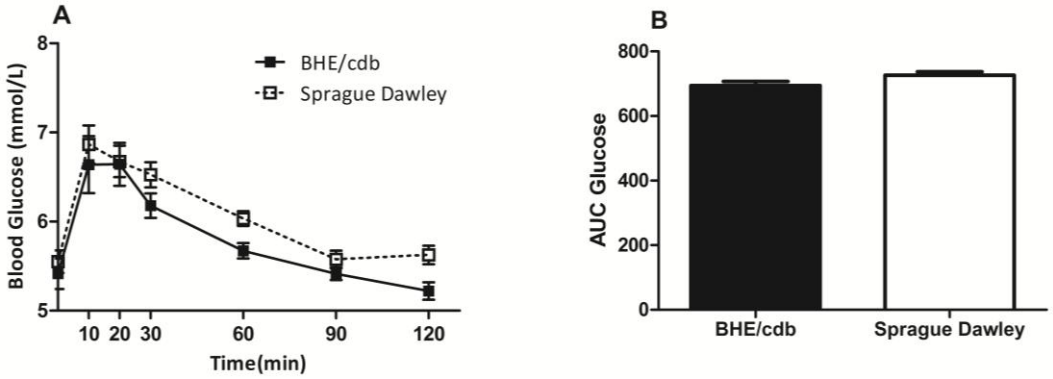

Figure 4.7- Intraperitoneal pyruvate tolerance test (2mg/kg sodium pyruvate). BHE/cdb n=14, SD n=12. (A)Blood glucose over the course of PTT: 2-way ANOVA shows overall BHE/cdb group has lower blood glucose than SD rats ($p<0.01$). (B) Net glucose area under the curve: Student's t-test shows no difference between groups ($p=0.073$).

4.3 Immunoblotting in Liver and Skeletal Muscle

Liver, slow-twitch soleus muscle, and fast-twitch epitrochlearis muscle lysates from standard chow fed rats were analyzed in order to measure total expression and phosphorylation of key proteins involved in peripheral glucose homeostasis, including insulin-dependent and insulin-independent signaling pathways. The liver is a central regulator of glucose homeostasis, especially gluconeogenesis, in the body, while the muscle is responsible for approximately 70%-90% of insulin-stimulated glucose uptake (Biddinger & Kahn, 2006).

As expected, insulin stimulation rapidly increased overall Akt phosphorylation at serine 473 in liver (*$p<0.01$), but there was no differential effect of genotype on Akt activation (Figure 4.8A). Insulin stimulation did not affect the phosphorylation state of insulin-independent signaling marker AMPK, as expected. However, there was also no effect of genotype on pAMPK expression in either the fasted or fed state (Figure 4.8B,C). Following the results of AMPK activation, there were no differences in its downstream signaling target pACC in either the fed or fasted state (Figure 4.8D,E). While there were no differences detected in phosphorylation of liver signaling pathways, total PEPCK expression, the rate limiting enzyme in liver gluconeogenesis, was decreased in BHE/cdb rats by approximately 35% in the fasted state (*$p<0.05$) and 30% in the fed state (*$p<0.001$) as compared to SD rats, suggesting decreased liver gluconeogenesis (Figure 4.8E). The decreased expression of PEPCK correlates with the decreased blood glucose in BHE/cdb rats previously seen in the pyruvate tolerance tests.

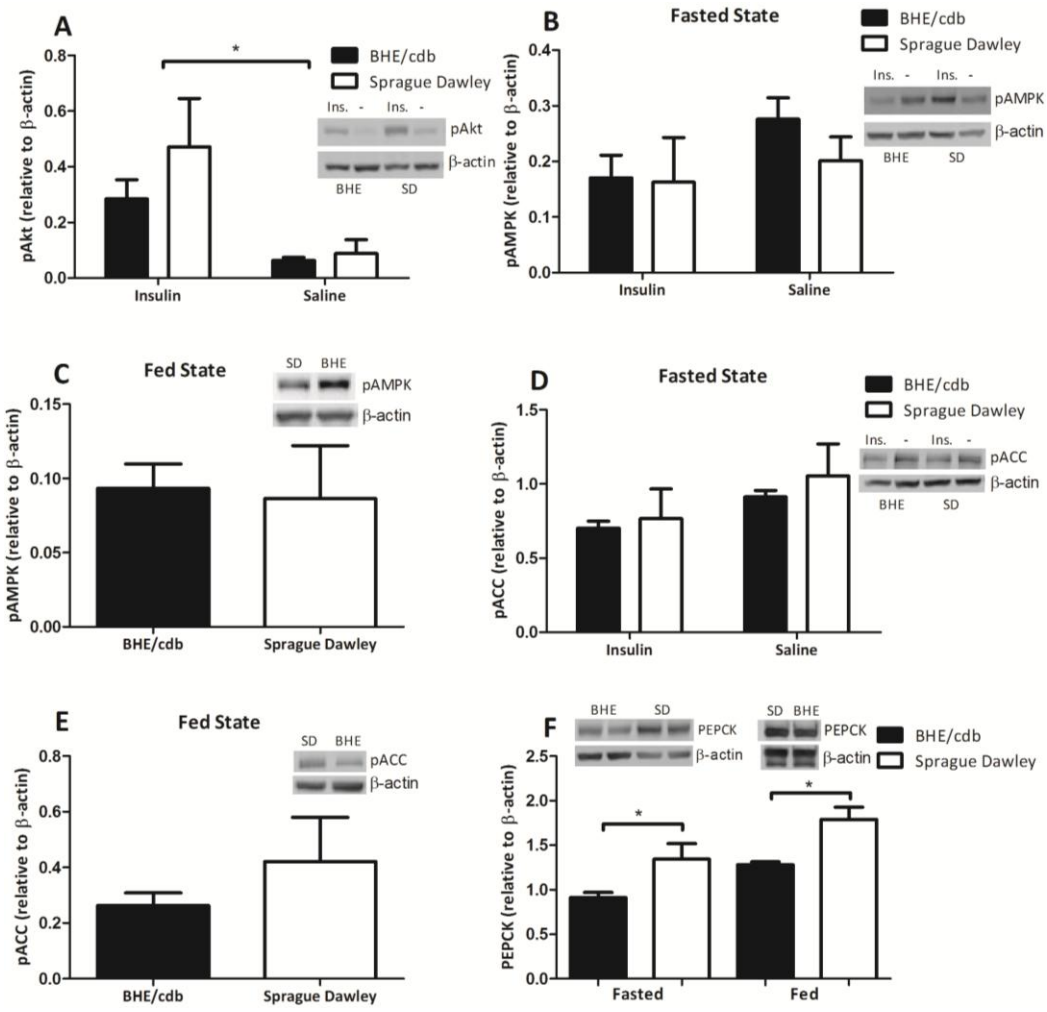

Figure 4.8-Immunoblotting in liver of chow fed rats. (A) pAkt expression in the fasted state (BHE/cdb n=6, SD n=4). Insulin significantly increased Akt phosphorylation (*p<0.01), with no effect of genotype (p=0.23). (B) Fasted state pAMPK (BHE/cdb n=6, SD n=4) expression was not affected by insulin (p=0.17) or rat genotype (p=0.43). (C) Fed state pAMPK (BHE/cdb n=9, SD n=3) was not different between BHE/cdb rats and SD rats (p=0.83). (D) pACC fasted state (BHE/cdb n=6, SD n=4) expression showed no difference due to insulin (p=0.06) or genotype (p=0.41). (E) Similarly, pACC fed state (BHE/cdb n=7, SD n=2) expression is similar in both groups (p=0.07). (F) PEPCK expression in BHE/cdb rats is significantly blunted compared to SD rats in both fasted (BHE/cdb n=12, SD n=8; *p<0.05) and fed state animals (BHE/cdb n=9, SD n=3; *p<0.001).

Skeletal muscle tissue also plays a significant role in whole-body glucose homeostasis. The expression and activation of GLUT 4, the main skeletal muscle glucose transporter protein, can be regulated by both insulin-dependent Akt signaling pathway and the insulin-independent signaling AMPK pathway (Taniguchi *et al.,* 2006; Long & Zierath, 2006). In soleus muscle tissue, genotype did not affect total GLUT 4 expression in either fasted or fed state rats (Figure 4.9A,B). Interestingly, insulin stimulated Akt phosphorylation in fasted state soleus muscle is significantly greater in SD as compared to BHE/cdb rats (*$p<0.01$), along with the expected overall significant effect of insulin on Akt phosphorylation (Figure 4.9C; #$p<0.01$). However, despite the overall significant effect of insulin, there was no difference between genotypes in epitrochlearis muscle tissue Akt phosphorylation. (Figure 4.10A; *$p<0.01$). Fasted state pAMPK expression in soleus (Figure 4.9D) and epitrochlearis muscle (Figure 4.10B) follows the same trend observed in liver tissue, with no significant effect of either insulin stimulation or genotype. Also similar to results seen liver protein expression, the expression of pACC in epitrochlearis tissue is not different in BHE/cdb rats as compared to SD rats, nor was any significant effect of short-term insulin stimulation detected (Figure 4.10C).

In order to determine if anti-oxidant mechanisms were up-regulated to compensate for proposed increases in oxidative stress in the BHE/cdb model, MnSOD expression (Figure 4.9E) and catalase expression (Figure 4.9F) was assessed in soleus muscle tissue lysates, but no difference were observed between BHE/cdb rats and SD rats. Additionally it should be noted that overall trends observed in fasted state protein expression were not different from trends of the same proteins measured in fed state animals.

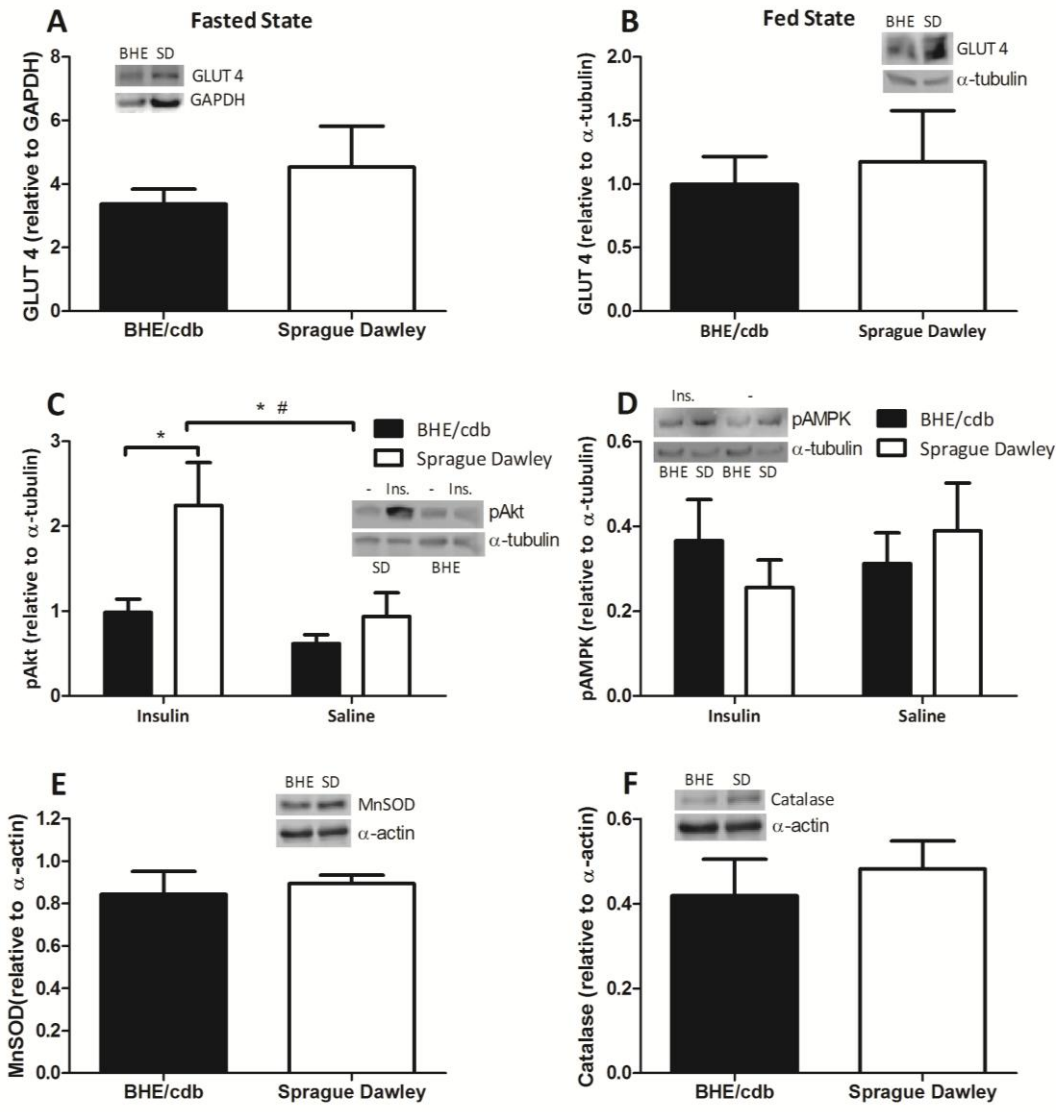

Figure 4.9- Immunoblotting in soleus muscle of chow fed rats. (A) No significant difference between BHE/cdb rats and SD rats in fasted state GLUT 4 expression (BHE/cdb n=8, SD n=5; p=0.34). (B) Similarly, genotype has no effect (p=0.69) on GLUT 4 expression in fed state animals (BHE/cdb n=9, SD n=3). (C) pAkt (Ser473) expression in the fasted state (BHE/cdb n=6, SD n=4) is significantly increased by insulin stimulation (#p<0.01) and is greater in SD rats compared to BHE/cdb rats (*p<0.01). (D) No effect of insulin stimulation (p=0.66) or genotype (p=0.86) on pAMPK expression was observed in fasted state rats. Fasted state expression of oxidative stress proteins (E) MnSOD (BHE/cdb n=8, SD n=5; p=0.73) and (F) catalase (BHE/cdb n=8, SD n=5; p=0.61) was not different between BHE/cdb rats and SD rats.

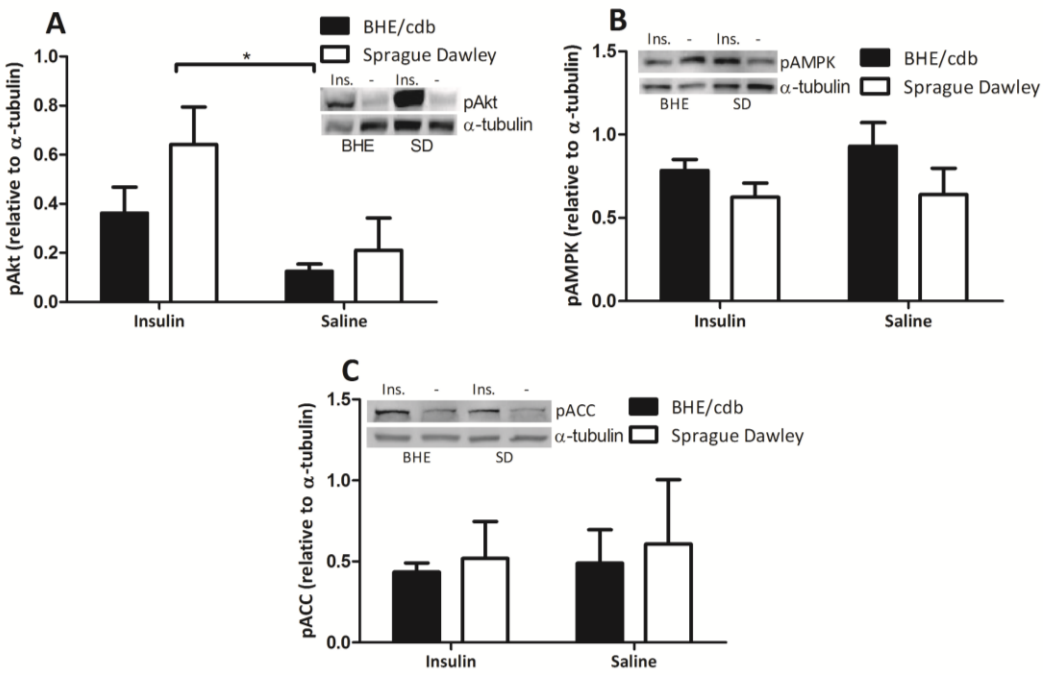

Figure 4.10 – Immunoblotting in epitrochlearis muscle of chow fed rats. BHE/cdb n=6, SD n=4. (A) pAkt (Thr 308) expression in fasted state. Overall, insulin is greater than saline (*p<0.01), with no effect of genotype (p=0.10). (B) Fasted state pAMPK expression levels show no effect of insulin (p=0.52) or genotype (p=0.08). (C) Fasted state pACC expression is not different for BHE/cdb rats compared to SD rats (p=0.66), with no insulin effect (p=0.75).

4.4 Transcription Factor Activation

Transcription factor activation was quantified from nuclear extracts from fasted liver and soleus muscle tissue to measure gene regulation of specific proteins of interest based on results from previous immunoblotting experiments. FOXO1 (forkhead box class O1) activation in liver is one of the main transcriptional regulators of PEPCK and gluconeogenesis (Puigserver *et al.,* 2003). However, despite differences in PEPCK protein expression seen in liver immunoblotting, the levels of FOXO1 activation in both liver and muscle nuclear extracts were similar for BHE/cdb and SD rats (Figure 4.11A). Mef2 (myocyte enhancer factor 2) is

involved in the transcriptional regulation of GLUT 4 (Thai *et al.,* 1998). No difference in Mef2 activation levels was detected in either soleus muscle extracts or liver extracts between bhe/cdb rats and SD rats (Figure 4.11B).

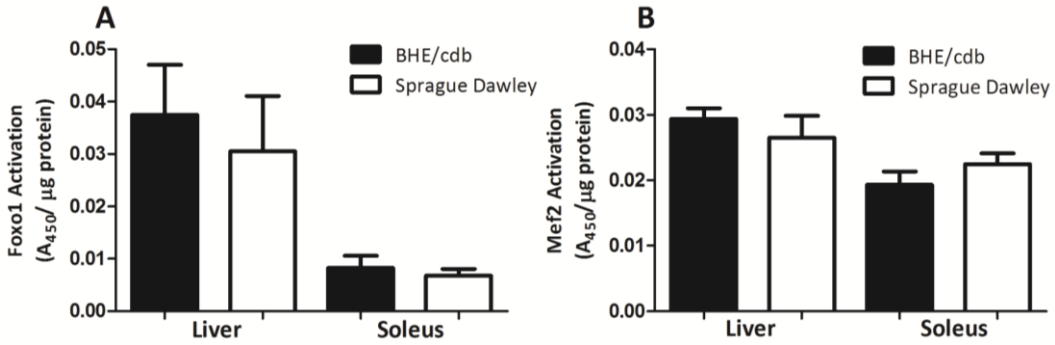

Figure 4.11 – Transcription factor activation. n=10 (A) FoxO1 transcription factor activation showed no differences between BHE/cdb rats and SD rats in liver (p=0.63) or soleus (p=0.58).in liver tissue. (B) Mef2 activation. In both liver tissue (p=0.45) and soleus muscle tissue (p=0.25) there were similar levels of transcription factor activation.

4.5 Tissue Composition Studies

Tissue glycogen content was measured using a colourimetric assay (Figure 4.12). Both liver ($p<0.05$) and epitrochlearis muscle tissue ($p<0.01$) had higher glycogen content in BHE/cdb rats as compared to age-matched SD rats. However, there was no difference in glycogen content of soleus muscle tissue (p=0.37).

The lipid composition of liver and slow-twitch soleus muscle was measured using gas chromatography (Table 4.2). There was no difference between BHE/cdb rats and SD rats in regards to either total lipid content in the tissues measured, or specific lipid type (monoglycerides, cholesterol, phospholipids, cholesterol esters and trigylcerides).

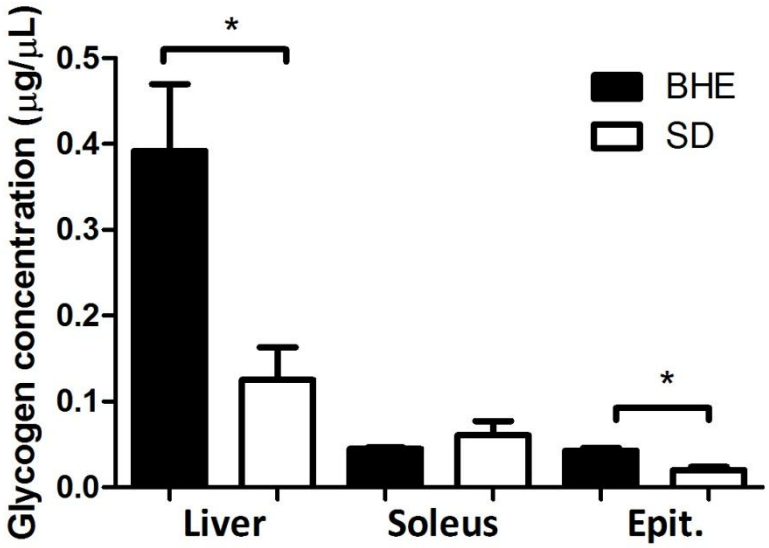

Figure 4.12 – Glycogen concentration in liver, soleus and epitrochlearis tissue of BHE/cdb rats compared to SD rats, using student's t-tests. Liver glycogen concentration is significantly higher in BHE/cdb rats (n=5) than SD rats (n=4) ($p < 0.05$). In soleus muscle there was no difference in tissue glycogen content between BHE/cdb and SD groups (n=5; p=0.37). Glycogen content in epitrochlearis muscle tissue was significantly higher in BHE/cdb group (n=5, $p<0.01$).

Table 4.2 – Lipid Composition of Liver and Soleus Tissue

μg lipid/mg protein	Liver			Soleus		
	BHE/cdb	SD	p value	BHE/cdb	SD	p value
Total Lipid	82.03 ± 6.5	82.72 ± 6.5	0.94	53.21 ± 7.23	41.44 ± 12.36	0.44
Monoglycerides	0.27 ± 0.04	1.14 ± 0.78	0.29	0.44 ± .05	0.51 ± 0.05	0.40
Cholesterol	7.50 ± 0.59	8.22 ± 0.61	0.42	3.70 ± 0.32	3.88 ± 0.28	0.69
Phospholipids	63.70 ± 5.7	64.07 ± 5.6	0.96	31.95 ± 4.6	24.23 ± 5.4	0.30
Cholesterol Esters	1.97 ± 0.37	1.06 ± 0.30	0.09	0.44 ± 0.35	0.33 ± 0.19	0.79
Triglycerides	8.58 ± 3.4	8.23 ± 2.6	0.93	16.67 ± 2.9	12.50 ± 6.8	0.60

Summary of lipid composition. n=5 for all groups. Student's t-tests show no significant differences in total lipid content or specific lipid type in liver or soleus tissues. Data are presented as mean ± SEM.

5.0 Discussion

Overall, it appears that the male BHE/cdb rats in our lab do not exhibit a diabetes-like phenotype as severe as previously described by Berdanier and colleagues (Berdanier, 2007; Berdanier, 1991). While there was evidence of blunted glucose-stimulated insulin secretion in males at 21 weeks (Figure 4.5), previous work in our lab demonstrated that male BHE/cdb rats did not develop impaired glucose tolerance up to 1 year of age (Saleh *et al.,* 2008). Additionally, in this project we found no evidence of excess lipid accumulation in the liver (Table 4.2), which has been described at characteristic of the strain (Berdanier, 2007; Berdanier, 1991). Normal glucose tolerance and insulin sensitivity have been reported at a similar age previously (Mathews *et al.,* 2000), but this is the first report of enhanced glucose clearance from the blood in response to a glucose load at 21 weeks of age in this strain. The origin of the mitochondrial diabetic phenotype is reported to occur as a result of mutations in mtDNA coding for the F_o subunit of ATP synthase (Mathews *et al.,* 1999). Differences in the overall phenotype seen in this project may be due to genetic drift in our colony. It is well known that mtDNA is highly susceptible to mutations (Wallace, 1999), and further mitochondrial mutations may have contributed to adaptations in our colony. However, genetic drift in the nuclear genome may also account for changes in peripheral glucose metabolism in our BHE/cdb colony. Such changes that may occur not only include genetic mutations, but may also involve epigenetic regulation of gene expression.

A preliminary investigation into the expression of antioxidant enzymes in muscle and liver tissue showed no differences between BHE/cdb and SD rats. These results may indicate, despite the limited parameters measured, that the generation of reactive oxygen species in peripheral tissues does not seem to play a large role

in peripheral glucose homeostasis. Additionally, we did not find an increase in activation of markers of insulin-independent AMPK signaling, nor in preferential activation of the insulin-dependent P13K-Akt signaling cascade in muscle. However, results indicate that increased metabolic rate, preferential oxidation of carbohydrates and decreased hepatic glucose output may contribute to enhanced glucose homeostasis in this model.

The overall relative body composition of BHE/cdb rats is similar when compared to SD rats. However, SD rats display a consistently higher body weight than BHE/cdb. Short-term feeding of a high fat diet did not significantly increase weight in either strain (Figure 4.1). These results are consistent with the lean and obesity resistant phenotype of BHE/cdb rats previously reported (Berdanier, 1991). The overall smaller mass in the BHE/cdb rats may be due to decreased energy availability as a result of lower ATP generation, thus contributing to growth stunting.. It should be noted that previous work in our lab has shown that when compared with both age-matched and weight-matched SD rats, the BHE/cdb rats display enhanced glucose tolerance, indicating that age-matched SD rats are a valid control (Chan, unpublished data). Further, results from this project show that despite a higher body weight in SD rats, there was no difference in relative fat and lean mass composition in chow-fed rats (Figure 4.2). This finding is inconsistent with early reports in non-obese BHE/cdb rats of decreased lean body mass and increased fat mass compared to normal rats (Berdanier, 1991). Additionally, in contrast to previously reported studies that characterize BHE/cdb rats as having a fatty liver as early as 7-14 weeks of age, there were no differences detected in total liver lipid accumulation or lipid type compared to SD controls (Berdanier, 1991;

Berdanier, 2007). Similarly, no lipid accumulation was observed in soleus muscle tissue (Table 4.3).

We originally hypothesized that increased fatty acid oxidation may occur as a result of a compensatory mechanism to decrease lipid accumulation in liver in order to subsequently enhance insulin sensitivity in the BHE/cdb rat (Zhou *et al.,* 2001; Berdanier, 2007). Decreasing or preventing muscle and liver intracellular lipid accumulation has been linked to increased insulin sensitivity (Samuel *et al.,* 2010). However, BHE/cdb rats consistently demonstrated a higher respiratory exchange ratio over the course of indirect calorimetry measurements (Figure 4.3 A), which corresponds to preferential oxidation of carbohydrates as compared to fat. When RER is near 1.0, carbohydrates are the primary oxidative source for energy, whereas when RER is approximately 0.7, fat is the main energy source (Choi *et al.,* 2007). Results showing higher RER in BHE/cdb rats could indicate that increased lipid oxidation is not required to maintain peripheral insulin sensitivity, because there was no evidence of excess whole body fat mass or accumulation of lipids in liver or muscle when compared to SD rats. Indeed, preferential utilization of glucose itself as an oxidative substrate could contribute to decreases in plasma glucose. Indirect calorimetry and metabolic monitoring has been used to evaluate diet and age-induced changes in BHE/cdb rats previously (Mathews *et al.,* 2000). Mathews and colleagues reported a tendency for a shift from nocturnal feeding to light-phase feeding by 150 days of age compared to SD control rats, while diurnal variations in food intake, activity and energy expenditure were normal for BHE/cdb and SD rats in our study (Figure 4.4). However, a similar trend for higher RER in BHE/cdb rats fed a stock diet compared to SD rats confirmed preferential glucose oxidation in BHE/cdb rats (Mathews, *et al.,* 2000).

Overall metabolic rate was higher in BHE/cdb rats, as is seen with consistently higher rates of carbon dioxide production and oxygen consumption (Figure 4.3 B/C). Heat production relative to body weight was also higher in BHE/cdb rats than in SD rats, which cannot be attributed to changes in physical activity, food or water consumption (Figure 4.3 D, Figure 4.4 & Table 4.1). However, subtle increases in physical activity and food intake that were not significant over the course of 24 hours may be significant if these parameters were measured over a longer period of time. Therefore, we cannot definitively exclude the possibility of behavioural differences in the long-term contributing to increased energy expenditure. Increased thermogenesis is indicative of uncoupling of oxidative phosphorylation and proton leak across the inner mitochondrial membrane. Mathews and colleagues (2000) also reported higher heat production relative to body weight in BHE/cdb rats compared to SD controls. Reduced efficiency of ATP synthesis in BHE/cdb rats due to the mitochondrial mutation could contribute to increased proton leak across the inner mitochondrial membrane (Berdanier & Thomson, 1986; Mathews *et al.,* 2000). Consequently, there would be an increase in energy released as heat rather than transferred into the high-energy bonds of ATP. Increased energy expenditure as a result of uncoupling has been shown to protect against lipid accumulation (Samuel *et al.,* 2010). Choi and colleagues (2007), have demonstrated that over-expression of muscle-specific uncoupling protein 3 (UCP3) protects against whole-body lipid-induced insulin resistance. Results from the UCP3 over-expression model, and other genetic models relating to uncoupling, indicate that an overall increase in energy expenditure due to uncoupling is responsible for improvements in insulin action, rather than a shift in oxidative substrate preference (Choi *et al.,* 2007; Samuel *et al.,* 2010).

As expected, enhanced glucose tolerance in chow-fed male BHE/cdb rats at 21 weeks-old was confirmed by enhanced glucose clearance from the blood despite significantly blunted insulin secretion (Figure 4.5). The results from ipGTTs are consistent with previous OGTTs conducted in our lab (Chan, unpublished data), but it should also be noted that in using an intraperitoneal injection of glucose, we are excluding the action of the gastrointestinal tract and gut-associated hormones on insulin secretion and glucose homeostasis. The incretin hormones, glucose-dependent insulinotropic polypeptide and glucagon-like peptide-1, both stimulate insulin secretion from the beta cells with high glucose concentrations in the gut (Baggio & Drucker, 2007). The effect of incretin hormones may account for some variations in insulin secretion and glucose homeostasis not examined in this project. While HFD did not significantly increase insulin secretion in BHE/cdb rats during the ipGTT when compared to their chow-fed counterparts (Figure 4.5C), glucose clearance in HFD BHE/cdb rats was normal (Figure 4.5A). These results indicate that as anticipated, upon the stress of high fat feeding, the protective effect on glucose tolerance in the BHE/cdb rat is lost. This is consistent with several previous reports that high-fat feeding exacerbates the development of impaired glucose tolerance and diabetes-like symptoms in BHE/cdb rats (Berdanier 1991, Berdanier *et al.,* 1992; Mathews *et al.,* 2000).

Enhanced glucose clearance may be attributed to enhanced insulin sensitivity exhibited in the insulin tolerance test of chow-fed rats (Figure 4.6). This is consistent with evidence showing that humans with mitochondrial disorders resulting in respiratory chain deficiency in skeletal muscle may have diabetes, but are not usually resistant to insulin action (Schiff *et al.,* 2009). Additionally, two carriers of the A3243G mt mutation have displayed increased insulin sensitivity

despite low insulin secretion (Maassen *et al.,* 2004). However, while there was an overall decrease of glucose in response to insulin in BHE/cdb rats compared to SD rats, the results of the ITT do not show enhanced insulin action *per se*. The first 30 minutes of an ITT are reflective of insulin action and the slope of the line can be used to interpret enhancements in insulin sensitivity in the body. However, the remaining time of the test reflects counter-regulatory actions to correct hypoglycemia (Alaya *et al.,* 2010). Thus, as there are no differences in the initial stages of the ITT, insulin action does not appear to be enhanced in the BHE/cdb model. Rather, glucose levels remain significantly lower in the latter portion of the ITT, an indication of diminished counter-regulatory response to low plasma glucose, which may be due to reduced hepatic glucose output.

The BHE/cdb model is comparable to a transgenic mouse model with tissue-specific knockout of the mitochondrial protein apoptosis inducing factor (AIF). The primary physiological role of AIF is the maintenance of a fully functional respiratory chain; therefore ablation of this protein leads to ATP deficiency, similar to the BHE/cdb rat (Pospisilik *et al.,* 2007). AIF muscle- and liver-specific knockout mice develop mild impairments in mitochondrial oxidative phosphorylation which can result in decreased cellular ATP and increased cellular AMP. Interestingly though, consistent with results seen in our study, AIF knockout mice show enhanced glucose tolerance upon OGTT despite reduced insulin secretion. Additionally, AIF knockout mice showed enhanced insulin sensitivity upon ITT, no change in ROS production, and were resistant to the development of diet-induced obesity (Pospisilik *et al.,* 2007). Likewise, a mouse model with muscle-specific knockout of mitochondrial transcription factor a, which results in a deficiency in skeletal muscle mitochondrial oxidative phosphorylation, does not develop insulin

resistance and shows increased peripheral glucose disposal in response to ipGTT (Wrendenberg *et al.,* 2006).

The liver is a critical hub of gluconeogenesis in the fasted state and overall glucose homeostasis in the body, and results indicate that it plays a central role in the enhanced glucose tolerance of the BHE/cdb model. Suggestions of reduced hepatic glucose output in the counter-regulatory phase of the ITT in BHE/cdb rats correlate with *in vivo* observations of reduced glucose output in response to pyruvate stimulation in the pyruvate tolerance test (Figure 4.7). Administration of the gluconeogenic substrate pyruvate increases blood glucose through stimulation of hepatic gluconeogenesis (Fukushima *et al.,* 2010). Correspondingly, expression of PEPCK, a rate limiting gluconeogenic enzyme, was significantly blunted in fed and fasted state liver tissues (Figure 4.8F). Additionally, fasted hepatic glycogen storage was increased when compared to controls (Figure 4.12). Reductions in the activity or expression of enzymes involved in glycogenolysis, such as glucose-6-phosphatase, may contribute to increased hepatic glycogen storage (Yabaluri & Bashyam, 2010). Previous reports indicate that BHE/cdb rats displayed increased liver glycogen stores, which is consistent with result in this study (Berdanier, 2001). However, in contrast to our results, gluconeogenesis was shown to be increased. Nevertheless, these results indicate that hepatic glucose output is reduced in BHE/cdb rats, and could therefore contribute to whole body glucose tolerance.

However, the specific molecular mechanisms regulating this compensatory mechanism in the BHE/cdb rat are unclear. Both AMPK- and Akt-mediated suppression of PEPCK expression involve the regulatory inhibition of the

transcription factor FoxO1 (Puigserver *et al.,* 2003; Koo *et al.,* 2005). Akt-mediated phosphorylation of FoxO1 sequesters it in the cytosol, while AMPK acts by indirectly inhibiting co-activator PGC-1α activity (Puigserver *et al.,* 2003; Koo *et al.,* 2005). However, FoxO1 activation, as measured in liver nuclear extracts, was similar in BHE/cdb and SD rats (Figure 4.11A). Although Akt phosphorylation was increased upon acute insulin stimulation, there was no difference in the extent of phosphorylation between BHE/cdb rats and SD rats (Figure 4.8A). Additionally, fed and fasted state expression of pAMPK and its downstream target pACC were not different between genotype in liver tissues (Figure 4.8B-E). There is evidence of impaired ATP synthesis in BHE/cdb hepatocytes (Berdanier & Thomson, 1986). Some pathways have been identified in which reduction of ATP reduced PEPCK and gluconeogenesis independent of insulin, but the treatment was shown to also reduce FoxO1 expression mediated through AMPK activation (Xia *et al.,* 2011). Further evidence has shown that low ATP can inhibit gluconeogenesis independent of AMPK activation and without transcriptional alteration of genes for PEPCK, possibly through alterations in gluconeogenic flux (Foretz *et al.,* 2010).

Measurements of Akt- and AMPK- dependent mechanisms in muscle did not reveal any significant differences in the BHE/cdb rat. Total expression of the facilitative glucose transporter GLUT 4, the main glucose transporter protein in muscle (Thai *et al.,* 1998), was not altered in the fed or fasted state soleus muscle tissue (Figure 4.9 A/B). Therefore, it follows that activation of the Mef2 transcription factor, which is responsible for transcriptional regulation of GLUT 4 protein expression (Thai *et al.,* 1998), was not changed in nuclear extracts of soleus muscle (Figure 4.11 B). However, whole-tissue western blot lysates are not representative of GLUT4 translocation to the membrane, nor did we measure the rate of glucose

uptake into isolated muscle tissue. Similar total GLUT4 expression seen in soleus muscle tissue does not necessarily preclude the presence of enhanced GLUT4 translocation or activity, which may contribute to increased glucose uptake into skeletal muscle (Merry & McConnell, 2009; Kurth-Kraczek *et al.,* 1999; Sano *et al.,* 2003).

As expected, and consistent with results seen in the liver, there was increased phosphorylation of Akt in insulin stimulated epitrochlearis and soleus muscle tissues in the fasted states (Figure 4.9C & Figure 4.10A). However, it is unclear why there was a subtle increase in SD muscle soleus tissue Akt phosphorylation that was not seen in epitrochlearis muscle. Akt-mediated signaling pathways were not expected to be significantly different, as the first phase responses seen in the insulin tolerance test were not different.

Theoretically, an increase in the AMP:ATP ratio would activate AMPK through thr172 phosphorylation and be representative of increased glucose translocation to the cellular membrane (LeBrasseur *et al.,* 2005). However, we did not detect any changes in pAMPK or its downstream target pACC in muscle tissues (Figure 4.9D & Figure 4.10B/C). In contrast to the results seen previously in female BHE/cdb islets (Saleh *et al.,* 2008), MnSOD expression in soleus muscle of BHE/cdb rats was similar to that seen in SD rats (Figure 4.9F). The mitochondrial antioxidant enzyme MnSOD converts superoxide to hydrogen peroxide and is up-regulated in β-cells in response to oxidative stress (Green *et al.,* 2004). Additionally, there was no difference in the level of catalase, an antioxidant enzyme that converts hydrogen peroxide to water (Merry & McConnell, 2009), in the BHE/cdb rats and the SD rats (Figure 4.9G). Normal ROS production is consistent with our results showing no

differences in AMPK phosphorylation in muscle and liver tissues, as increased ROS production has been associated with increased AMPK activation (Toyoda *et al.,* 2004).

Curiously, muscle-specific Tfam knockout mice did not display increased levels of GLUT 4 protein expression, total AMPK, or pAMPK in fast-twitch extensor digitorum longus (EDL) muscle or soleus muscle (Wrendenberg *et al.,* 2006). While AMPK phosphorylation state in Tfam muscle knockouts was not changed relative to controls, these authors did show an increase in the phosphorylation of downstream target ACC, which was not seen in our results in epitrochlearis fast-twitch muscle (Figure 4.10C) (Wrendenberg *et al.,* 2006). However, it was noted that measurement of AMPK phosphorylation does not account for allosteric activation of AMPK by increased AMP concentrations (Hegarty *et al.,* 2009; Wrendenberg *et al.,* 2006). Interestingly, there is some evidence that glycogen can also act as an allosteric regulator of AMPK and glucose transport (Merry & McConnell, 2009; Wrendenberg *et al.,* 2006). Glycogen stores in soleus muscle were not found to be different in BHE/cdb rats as compared to SD rats, but there was evidence of increased glycogen storage in epitrochlearis muscle (Figure 4.12). However, the mechanism by which glycogen storage may regulate muscle glucose transport is not yet clear, but it has been suggested that increased glycogen is inhibitory of glucose transport in fast-twitch muscle fibers (Merry & McConnell, 2009; Derave *et al.,* 2000). Increased muscle glycogen storage is also curious as insulin stimulates glycogen synthesis, and the BHE/cdb model has chronically low insulin secretion. Overall, when compared to liver, muscle does not appear to play as important a role in glucose tolerance in this model.

In summary, increased thermogenesis, preferential whole body oxidation of glucose, increased glycogen storage and reduced hepatic glucose output appear to be contributing factors to improved glucose homeostasis in the 21-week old male BHE/cdb rat model. Hepatic glucose regulation was altered, presumably as a compensatory mechanism due to impaired insulin secretion. Given that this study was not able to show changes in Akt-mediated or AMPK-mediated signaling pathways that could account for reduced PEPCK expression without a corresponding decrease in FoxO1 activation, further examinations of the molecular mechanisms involved in reduced hepatic glucose output are warranted. Recent work has questioned the efficacy of PEPCK expression on control of hepatic gluconeogenesis, indicating that evaluation of other key gluconeogenic enzymes in this model, such as glucose-6-phosphatase, would be useful (Ramnanan *et al.,* 2010). While this study did not detect large changes in parameters measured in muscle tissue, measurements of GLUT 4 translocation and actual glucose transport in isolated muscle strips could help shed some light on the role of muscle-mediated glucose uptake. Investigations into proton leak or uncoupling as related to the markedly increased thermogenesis in BHE/cdb rat could also provide further insight into compensatory mechanisms in peripheral glucose metabolism.

Preliminary experiments showed no differences in UCP3 expression in BHE/cdb and SD muscle tissues and decreased expression of uncoupling protein1 in brown adipose tissue (C.B. Chan, M.E. Harper & A.B. Thrush, unpublished data). Therefore, examination of other enzymes involved in the control of fuel oxidation is warranted. The pyruvate dehydrogenase (PDH) enzyme is a central regulator of energy oxidation, where its up-regulation increases glucose oxidation by irreversibly converting pyruvate into acetyl-CoA (Jeong & Harris, 2008). The

preferential oxidation of carbohydrates observed in this study may be attributed to increased PDH activity. PDH is mainly regulated though inhibitory phosphorylation by pyruvate dehydrogenase kinases, and re-activated though dephosphorylation by pyruvate dehydrogenase phosphatases. Recent work has shown that reductions in pyruvate dehydrogenase kinase 4, a PDH inhibitor, improve glucose tolerance in diet-induced obesity (Leong & Harris, 2008). Examination of PDH and its regulators could help clarify compensatory mechanisms involving glucose oxidation in the BHE/cdb model.

Finally, evaluation of the impact of HFD, which was briefly assessed in this project, would be useful to determine how high fat feeding changes activation of peripheral signaling pathways. Several studies by Berdanier and colleagues indicate that HFD exacerbates the diabetic phenotype in the BHE/cdb model (Mathews et al., 2000; Berdanier 1991; Berdanier 2007). The type of fat fed has also been shown to influence function in the BHE/cdb rat. Diets consisting of primarily saturated fat worsen the efficiency of ATP synthesis in the BHE/cdb rat, whereas a diet containing primarily unsaturated fat improves mitochondrial function (Kim & Berdanier, 1998). In this project we showed that glucose tolerance worsened in the BHE/cdb rats upon feeding a high saturated fat diet, while insulin secretion remained blunted. However, changes in peripheral tissue molecular activation have not been evaluated with high fat feeding.

Further work remains to be done to determine the precise molecular mechanisms mediating glucose tolerance in the 21 week old male BHE/cdb rat. The results of this study, along with results from other models of impaired mitochondrial function such as Tfam knockout and AIF knockout mice (Silva *et al.,* 2000;

Wrendenberg *et al.,* 2006; Pospisilik *et al.,* 2007), indicate that further research into the relationship between mild impairments in mitochondrial oxidative phosphorylation and enhanced peripheral insulin sensitivity may lead to insights in novel methods for treating type 2 diabetes mellitus in the human population.

6.0 Literature Cited

Ayala, J.E.; Samuel, V.T.; Morton, G. J.; Obici, S.; Croniger, C.M.; Shulman, G.I.; Wasserman, D.H.; & McGuinness, O.P.; for the NIH Mouse Metabolic Phenotyping Center Consortium. (2010). Standard operating procedures for describing and performing metabolic tests of glucose homeostasis in mice. *Disease Models & Mechanisms,* 3*(9-10)*: 525-534.

Avurch, J. (1998). Insulin signal transduction through protein kinases. *Molecular and Cellular Biochemistry,* 182*(1-2)*:31-48.

Baggio, L.L. & Drucker, D.J. (2007). Biology of incretins: GLP-1 and GIP. *Gastroenterology,* 132*(6)*:2131-2157.

Berdanier, C.D. (1991). The BHE rat: an animal model for the study of non-insulin-dependent diabetes mellitus. *FASEB Journal,* 5*(8)*: 2139-2144.

Berdanier, C.D. (2001). Diabetes and nutrition: The mitochondrial part. *The Journal of Nutrition,* 131*(2)*:344S-353S.

Berdanier, C.D. (2007). Linking mitochondrial function to diabetes mellitus: an animal's tale. *American Journal of Physiology: Cell Physiology,* 293*(3)*:C830-C836.

Berdanier, C.D.; Johnson, B.; Hartle, D.K. & Crowell, W. (1992). Life span is shortened in BHE/cdb rats fed a diet containing 9% menhaden oil and 1% corn oil. *Journal of Nutrition,* 122*(6)*:1309-1317.

Berdanier, C.D. & Thomson, A.R. (1986). Comparative studies on mitochondrial respiration in four strains of rats (Rattus norvegicus). *Comparative Biochemistry and Physiology. B. Comparative Biochemistry,* 85*(3)*: 531-535.

Biddinger, S.B. & Kahn, R.C. (2006). From mice to men: Insights into the insulin resistance syndromes. *Annual Review of Physiology,* 68:123-158.

Brandle, M.; Lehmann, R.; Maly, F.E.; Schmid, C. & Spinas, G.A. (2001). Diminished insulin secretory response to glucose but normal insulin and glucagon secretory responses to arginine in a family with maternally inherited diabetes and deafness caused by mitochondrial tRNA (LEU(UUR)) gene mutation. *Diabetes Care,* 24*(7)*: 1253-1258.

Canadian Diabetes Association Clinical Practice Guidelines Expert Committee. (2008). Canadian Diabetes Association 2008 clinical practice guidelines for the prevention and management of diabetes in Canada. *Canadian Journal of Diabetes*, 32*(suppl 1):*S1-S201.

Cartee, G.D. & Wojtaszewski, J.F. (2007). Role of Akt substrate of 160 kDa in insulin-stimulated and contraction-stimulated glucose transport. *Applied Physiology, Nutrition & Metabolism,* 32*(3)*:557-66.

Cheatham, B.; Vlahos, C.J.; Cheatham, L.; Wang, L.; Blenis, J. & Kahn, C.R. (1994). Phosphatidylinositol 3- kinase activation is required for insulin stimulation of p70 S6 kinase, DNA synthesis, and glucose transporter translocation. *Molecular and Cellular Biology,* 14*(*7*):*4902-4911.

Cherrington, A.D. (1999). Banting lecture 1997: Control of glucose uptake and release by the liver in vivo. *Diabetes,* 48*(5)*:1198-1214.

Choi, C.S.; Fillmore, J.J.; Kim, J.K.; Liu, Z.-X.; Kim, S.; Collier, E.F.; Kulkarni, A.; Distefano, A.; Hwang, Y.-U.; Kahn, M.; Chen, Y.; Yu, C.; Moore, I.K.; Reznick, R.M.; Higashimori, T.; & Shulman, G. I. (2007). Overexpression of uncoupling protein 3 in skeletal muscle protects against fat-induced insulin resistance. *Journal of Clinical Investigation,* 117*(7)*: 1995-2003.

Cross, D.A; Alessi, D.R.; Cohen, P.; Andjelkovich, M. & Hemmings, B.A. (1995). Inhibition of glycogen synthase kinase-3 by insulin mediated by protein kinase B. *Nature,* 378*(6559)*:785-789.

de Andrade, P.B.M.; Rubi, B.; Frigero, F.; van den Ouweland, J.M.W., Masseen, J.A. & Maechler, P. (2006). Diabetes-associated mitochondrial DNA mutation A3243G impaires cellular metabolic pathways necessary for beta cell function. *Diabetologia,* 49 *(8):* 1816-1826.

DeFronzo, R.A.; Gunnarson, R.; Bjorkman, O.; Olson, M. & Wahren, J. (1985). Effects of insulin on peripheral and splanchnic glucose metabolism in noninsulin-dependent (type II) diabetes mellitus. *Journal of Clinical Investigation,* 76*(1)*:149-155.

Derave, W.; Ai, H.; Ihlemann, J.; Witters, L.A.; Kristiansen, S.; Richter, E.A. & Ploug, T. (2000). Dissociation of AMP-activated protein kinase activation and glucose transport in contracting slow-twitch muscle. *Diabetes,* 49*(8)*:1281-1287.

Doria, A.; Patti, M.-P. & Kahn, R.C. (2008). Review: The Emerging Genetic Architecture of Type 2 Diabetes. *Cell Metabolism*, (*8)*186-200.

Everts, H.B. & Berdanier, C.D. (2002). Nutrient-gene interactions in mitochondrial function: Vitamin A needs are increased in BHE/cdb rats. *IUBMB Life,* 53*(6)*:289-284.

Foretz, M.; Hébrard, S.; Leclerc, J.; Zarrinpashneh, E.; Soty, M.; Mithieux, G.; Sakamoto, K.; Andreelli, F. & Viollet, B. (2010). Metformin inhibits gluconeogenesis in mice independently of the LKB1/AMPK pathway via a decrease in hepatic energy state. *Journal of Clinical Investigation,* 120*(7)*: 2355- 2369.

Fukushima, A.; Loh, K.; Galic, S.; Fam, B.; Shields,B.; Wiede, F.; Tremblay, M.L.; Watt, M.J.; Andrikopoulos, S.; & Tiganis, T. (2010). T-cell protein tyrosine phosphatase attenuates STAT3 and insulin signaling in the liver to regulate gluconeogenesis. *Diabetes.* 59*(8)*: 1906-1914.

Green, K.; Brand, M. & Murphy, M.P. (2004). Prevention of mitochondrial oxidative damage as a therapeutic strategy in diabetes. *Diabetes,* 53*(Suppl 1)*: S110-S118.

Hawley, S.A.; Pan, D.A.; Mustard, K.J.; Ross, L.; Bain, J.; Edelman, A.M.; Frenquelli, B.G. & Hardie, D.G. (2005). Calmodulin-dependent protein kinase kinase-β is an alternative upstream kinase for AMP-activated protein kinase. *Cell Metabolism,* 2*(1)*:9-19.

Hegarty, B.D.; Turner, N.; Cooney, G.J. & Kraegen, E.W. (2009). Insulin resistance and fuel homeostasis: the role of AMP-activates protein kinase. *Acta Physiologica,* 196*(1)*: 129-145.

Higaki, Y.; Mikami, T.; Fujii, N.; Hirshman, M.F.; Koyama, K.; Seino, T.; Tanaka, K. & Goodyear, L.J. (2008). Oxidative stress stimulates skeletal muscle glucose uptake through a phosphatidylinositol 3-kinase-dependent pathway. *American Journal of Physiology, Endocrinology and Metabolism.* 294(*5):* E889-E897.

Jeong, N.H. & Harris, R.A. (2008). Pyruvate dehydrogenase kinase-4 deficiency lowers blood glucose and improves glucose tolerance in diet-induced obese mice. *American Journal of Phsyiology: Endocrinology & Metabolism,* 295*(1)*: E46-E54.

Kahn, C. R. (2003). Knockout mice challenge our concepts of glucose homeostasis and the pathogenesis of diabetes. *Experimental Diabesity Research,* 4*(3)*:196-182.

Karlsson, H.K.; Chibalin, A.V.; Koistinen, H.K.; Yang, J.; Koumanov, F.; Wallberg-Henriksson, H.; Zierath, J.R. & Holman, G. D. (2009). Kinetics of GLUT 4 trafficking in rat and human skeletal muscle. *Diabetes,* 58*(4)*:847-854.

Kennedy, E.D.; Maechler, P.E. & Wollheim, C.B. (1998). Effects of depletion of mitochondrial DNA in metabolism secretion coupling in INS-1 cells. *Diabetes,* 47*(3)*: 374-380.

Kim, M.-J.C. & Berdanier, C.D. (1998). Nutrient-gene interactions determine mitochondrial function: effect of dietary fat. *FASEB Journal,* 12*(2)*:243-248.

Kim, M.-J.; Ryu, G.R.; Kang, J.-H.; Sim, S.S.; Min, D.S.; Rhie, D.J.; Yoon, S.H.; Hahn, S.J.; Jeong, I.K.; Hong, K.J.; Kim, M.S.; & Jo, Y.H. (2004). Inhibitory effects of epicatechin on interleukin-1β-induced inducible nitric oxide synthase expression in RINm5F cells and rat pancreatic islets by down-regulation of NF-kappaB activation. *Biochemical Pharmacology,* 68*(9)*:1775-1785.

Koo, S.H.; Flechner, L.; Qi, L.; Zhang, X.; Screaton, R.A.; Jeffries, S.; Hedrick, S.; Xu, W.; Boussouar, F.; Brindle, P.; Takemori, H. & Montiminy, M. (2005). The CREB coactivator TORC2 is a key regulator of fasting glucose metabolism. *Nature,* 437*(7062)*:1109-1114.

Kurth-Kraczek, E.J.; Hirshman, M.F.; Goodyear, L.J. & Winder, W.W. (1999). 5`AMP-activated protein kinase causes GLUT 4 translocation in skeletal muscle. *Diabetes,* 48*(8)*: 1667-1671

LeBrasseur, N.K.; Kelly, M.; Tsao, T.-S.; Farmer, S.R.; Saha, A.K.; Ruderman, N.B. & Thomas, E. (2006). Thiazolidinediones can rapidly activate AMP-activated protein kinasein mammalian tissues. *American Journal of Physiology: Endocrinology and Metabolism,* 291*(1)*: E175-E181.

Li, X.; Monks, B.; Ge, O. & Birbaum, J.M. (2007). Akt/PKB regulated hepatic glucose metabolism by directly inhibiting PGC-1alpha transcription coactivator. *Nature,* 447*(7147)*: 1012-1016.

Liang, Y.; Bonner-Weir, S.; Wu, Y.-J.; Berdanier, C.D.; Berner, D.K.; Efrat, S. & Matchinsky, F.M. (1994). In situ glucose uptake and glucokinase activity of pancreatic islets in diabetic and obese rodents. *Journal of Clinical Investigation.* 93*(6)*: 2473-2481.

Long, Y.C. & Zierath, J.R. (2006). AMP-activated protein kinase signaling in metabolic regulation. *Journal of Clinical Investigation,* 116 *(7)*:1776-1782.

Maassen, J. A. (2002). Mitochondrial diabetes: Pathophysiology, clinical presentation, and genetic analysis. *American Journal of Medical Genetics: Seminars in Medical Genetics,* 115*(1)*:66-70.

Maassen, J.A.; Janssen, M.C. & 'T Hart, L.M. (2005). Molecular mechanisms of mitochondrial diabetes(MIDD). *Annals of Medicine,* 37*(3)*:213-222.

Maassen, J.A. & Kadowaki, T. (1996) Maternally inherited diabetes and deafness syndrome: a new diabetes subtype. *Diabetologia,* 39(*4*):375-382.

Maassen, J.A.; 't Hart, L.M.; van Essen, E.; Heine, R.J.; Nijpels, G.; Tafrechi, R.S.J.; Raap, A.K.; Janssen, G.M.C. & Lemkes, H.H. (2004). Mitochondrial diabetes: molecular mechanisms and clinical presentation. *Diabetes,* 53*(Suppl 1)*:S103-S109.

Mathews, C.E.; McGraw, R.A. & Berdanier, C.D. (1995). A point mutation in the mitochondrial DNA of diabetes-prone BHE/cdb rats. *FASEB Journal,* 9*(15)*: 1638-1642

Mathews, C.E.; McGraw, R.A.; Dean, R. & Berdanier, C.D. (1999). Inheritance of a mitochondrial DNA defect and impaired glucose tolerance in the BHE/cdb rats. *Diabetologia,* 42*(1)*:35-40.

Mathews, C.E.; Wickwire, K.; Flatt, W.P. & Berdanier, C.D. (2000). Attenuation of circadian rhythms of food intake and respiration in aging diabetes-prone BHE/cdb rats. *American Journal of Physiology. Regulatory, Integrative, and Comparative Physiology,* 279*(1)*:R230-238.

Matschinsky, F.M. (1996). Banting lecture 1995: A lesson in metabolic regulation inspired by the glucokinase glucose sensor paradigm. *Diabetes,* 45*(2)*:223-241.

McGee, S.L.; Van Denderen, B.; Howlett, K.; Mollica, J.; Schertzer, J.; Kemp, B. & Hargreaves, M. (2008). AMP-activated protein kinase regulates GLUT4 transcription by phosphorylating histone deacetylase 5. *Diabetes,* 57*(4)*:860-867.

Mclean, J.A. & Tobin, G. (1987). Animal and Human Calorimetry. Cambridge University Press, pp. 352. ISBNO-521-30905-0

Park, C.B. & Larsson, N.G. (2011). Mitochondrial DNA mutations in disease and aging. *Journal of Cell Biology,* 193*(5)*:809-819.

Pospisilik, J.A.; Knauf, C,; Joza, N.; Benit, P.; Orthofer, M.; Cani, P.D.; Ebersberger, I.; Nakashima, T.; Sarao, R.; Neely, G.; Esterbauer, H.; Kozlov, A.; Kahn, C.R.; Kroemer, G.; Rustin, P.; Burcelin, R. & Penninger, J.M. (2007). Targeted deletion of AIF decreases mitochondrial oxidative phosphorylation and protects from obesity and diabetes. *Cell*, 131*(3)*:476-491.

Puigserver, P.; Rhee, J.; Donovan, J.; Walkey, C.J.; Yoon, J.C.; Oriente, F.; Kitamura, Y.; Altomonte, J.; Dong, H.; Accili, D. & Spiegleman, B.M. (2003). Insulin-regulated hepatic gluconeogenesis through FOXO1-PGC-1α interaction. *Nature,* 293*(6939)*:550-555.

Roden, M.; Petersen, K.F. & Shulman, G.I. (2001). Nuclear magnetic resonance studies of hepatic glucose metabolism in humans. *Recent Progress in Hormone Research,* 56: 219-237.

Saha, A.K. & Ruderman, N.B. (2003). Malonyl-CoA and AMP-activated protein kinase: an expanding partnership. *Molecular and Cellular Biochemistry,* 253*(1-2)*:65-70.

Saleh, M.C.; Fatehi-Hassanabad, Z.; Wang, R.; Nino-Fong, R.; Wadowska, D.W.; Wright, G.M.; Harper, M.E. & Chan, C.B. (2008). Mutated ATP synthase induces oxidative stress and impaired insulin secretion in β-cells of female BHE/cdb rats. *Diabetes/Metabolism Research and Reviews,* 24*(5)*:392-403.

Samuel, V.T.; Petersen, K.F. Shulman, G.I. (2010). Lipid-induced insulin resistance: unraveling the mechanism. *Lancet,* 375*(9733)*: 2267-2277.

Sano, H.; Kane, S.; Sano, E.; Milnea, C.P.; Asara, J.M.; Lane, W.S.; Garner, C.W. & Lienhardm G. E. (2003). Insulin-stimulated phosphorylation of a Rab GTP-ase-activating protein regulates GLUT4 translocation. *Journal of Biological Chemistry,* 278*(17)*:14599-14602.

Schiff, M.; Loublier, S.; Coulibaly, A.; Benit, P.; Ogier de Baulny, H. & Rustin, P. (2009). Mitochondria and diabetes mellitus: untangling a conflictive relationship? *Journal of Inherited Metabolic Disease, (32)*684-698.

Shaw, R.J.; Lamia, K.A.; Vasquez, D.; Koo, S.H.; Bardeesy, N.; DePhinho, R.A.; Montminy, M. & Cantley, L.C. (2005). The kinase LKB1 mediates glucose homeostasis in liver and therapeutic effects of metformin. *Science,* 310*(5754)*:1642-1646

Silva, J.P.; Kohler, M.; Graff, C.; Oldfors, A.; Mgnuson, M.A.; Berggren, P.-O. & Larsson, N.-G. (2000). Impaired insulin secretion and β-cell loss in tissue specific knockout mice with mitochondrial diabetes. *Nature Genetics,* 26*(3)*:336-340.

Smith, P. K.; Krohn, R. I.; Hermanson, G. T.; Mallia, A. K.; Gartner, F. H.; Provenzano, M. D.; Fujimoto, E.K.; Goeke, N.M.; Olson, B.J. & Klenk, D.C. (1985). Measurement of protein using bicinchoninic acid. *Analytical Biochemistry, 150*(1), 76-85.

Sutherland, L.N.; Capozzi, L.C.; Turchinsky, N.J.; Bell, R.C. & Wright, D.C. (2008). Time course of high-fat diet-induced reductions in adipose tissue mitochondrial proteins: potential mechanisms and the relationship to glucose tolerance. *American Journal of Physiology, Endocrinology and Metabolism,* 295*(5)*:E1076-E1083.

Taniguchi, C.M.; Emanuelli, B. & Kahn, R.C. (2006). Critical nodes in insulin signaling pathways: insights into insulin action. *Nature Reviews: Molecular Cell Biology,* 7*(2)*:85-96.

Thai, M.V.; Guruswamy, S.; Cao, K.T.; Pessin, J.E.; Olson, A.L. (1998). Myocyte enhancer factor 2 (MEF2)-binding site is required for *GLUT4* gene expression in transgenic mice. *Journal of Biological Chemistry*, 273*(5)*:14885-14292.

Toyoda, T.; Hayashi, T,; Miyamoto, L.; Yonemitsu, S.; Nakano, M.; Tanaka, S.; Ebihara, K.; Masuzaki, H.; Hosoda, K.; Inoue, G.; Otaka, A,; Sato, K,; Fushiki, T.; & Nakao, K. (2004). Possible involvement of the alpha1 isoform of 5'AMP-activated protein kinase in oxidative stress-stimulated glucose transport in skeletal muscle. *American Journal of Physiology, Endocrinology and Metabolism,* 287*(1)*: 166-173.

van den Ouweland, J.M.; Lemkes, H.H.; Ruitenbeek, W.; Sandkuijl L.A.; Struvvenberg, P.A.; van de Kamp, J.J. & Maassen, J.A. (1992). Mutation in mitochondrial tRNA(Leu)(UUR) gene in a large pedigree with maternally transmitted type II diabetes mellitus and deafness. *Nature Genetics,* 1 *(5)*:368-371.

van Elderen, S.G.; Doornbos, J.; van Essen, E.H.; Lemkes, H.H., Maassen, J.A.; Smit, J.W. & de Roos, A. (2009). Phosphorus-31 magnetic resonance spectroscopy of skeletal muscle in maternally inherited diabetes and deafness A3243G mitochondrial mutation carriers. *Journal of Magnetic Resonance Imaging,* 29*(1)*:127-131.

Vazquez-Memije, M.E.; Shanske, S.; Sanlorelli, F.M.; Kranz-Eble, P.; DeVivo, D.C. & DiMaurro, S. (1998). Comparative biochemical studies of ATPase in cells from patients with T8993G or T8993C mitochondrial mutations. *Journal of Inherited Metabolic Disease,* 21*(8)*:829-836.

Wallace, D.C. (1999). Mitochondrial diseases in man and mouse. *Science,* 283*(5407)*:1482-1488.

Wrendenberg, A.; Freyer, C.; Sandstrom, M.E.; Katz, A.; Wibom, R.; Westerblad, H. & Larsson, N.G. (2006). Respiratory dysfunction in skeletal muscle does not cause insulin resistance. *Biochemical and Biophysical Research Communications,* 350*(1)*: 202-207

White, M.F. & Kahn, R.C. (1994). The insulin signaling system. *Journal of Biological Chemistry,* 269*(1)*:1-4.

Whiting, D.R.; Guariguata, L.; Weil, C.; & Shaw, J. (2011). "IDF Diabetes Atlas: Global estimates of the prevalence of diabetes for 2011 and 2030". *Diabetes Research and Clinical Practice*. 94(3):311-321.

Xia, X.; Yan, J.; Shen, Y.; Tang, K.; Yin, J.; Zhang, Y.; Yang, D.; Liang, H.; Ye, J. & Weng, J. (2010). Berberine improves glucose metabolism in diabetic rats by inhibition of hepatic gluconeogenesis. *PLoS One,* 6*(2)*: e16556.

Yabaluri, N. & Bashyam, M.B. (2009). Hormonal regulation of gluconeogenic gene transcription in the liver. *Journal of Biosciences,* 35*(3)*: 472-484.

Zhou, G.; Myers, R.; Li, Y.; Chen, Y.; Shen, X.; Fenyk-Melody, J.; Wu, M.; Ventre, J.; Doebber, T.; Fujii, N.; Musi, N.; Hirshman, M.F.; Goodyear, L.J. & Moller, D.E. (2001). Role of AMP-activated protein kinase in mechanism of metformin action. *Journal of Clinical Investigation,* 108*(8)*:1167-1174.